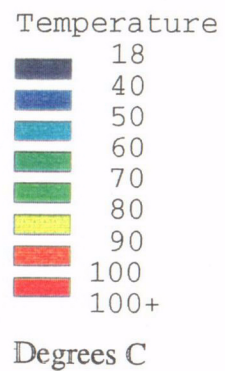


ANSYS 5.0 A
JAN 25 1995



21 PWR WP
Mid-plane
Temperatures

25 MTU/acre
(16.2 m WP Spacing)
(90 m Drift Spacing)

22 year old SNF
42.2 GWd/MTU

C15



Figure 6.2.12 Low Temperature Fuel Element (LE) Assembly

B00000000-01717-5705-00027 REV 00

6.2-25

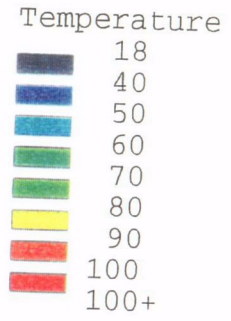
March 1996

ANSYS 5.0 A
JAN 25 1995

B00000000-01717-5705-00027 REV 00

6.2-27

March 1996



Degrees C

21 PWR WP
Mid-plane
Temperatures

25 MTU/acre
(16.2 m WP Spacing)
(90 m Drift Spacing)

22 year old SNF
42.2 GWd/MTU

C16

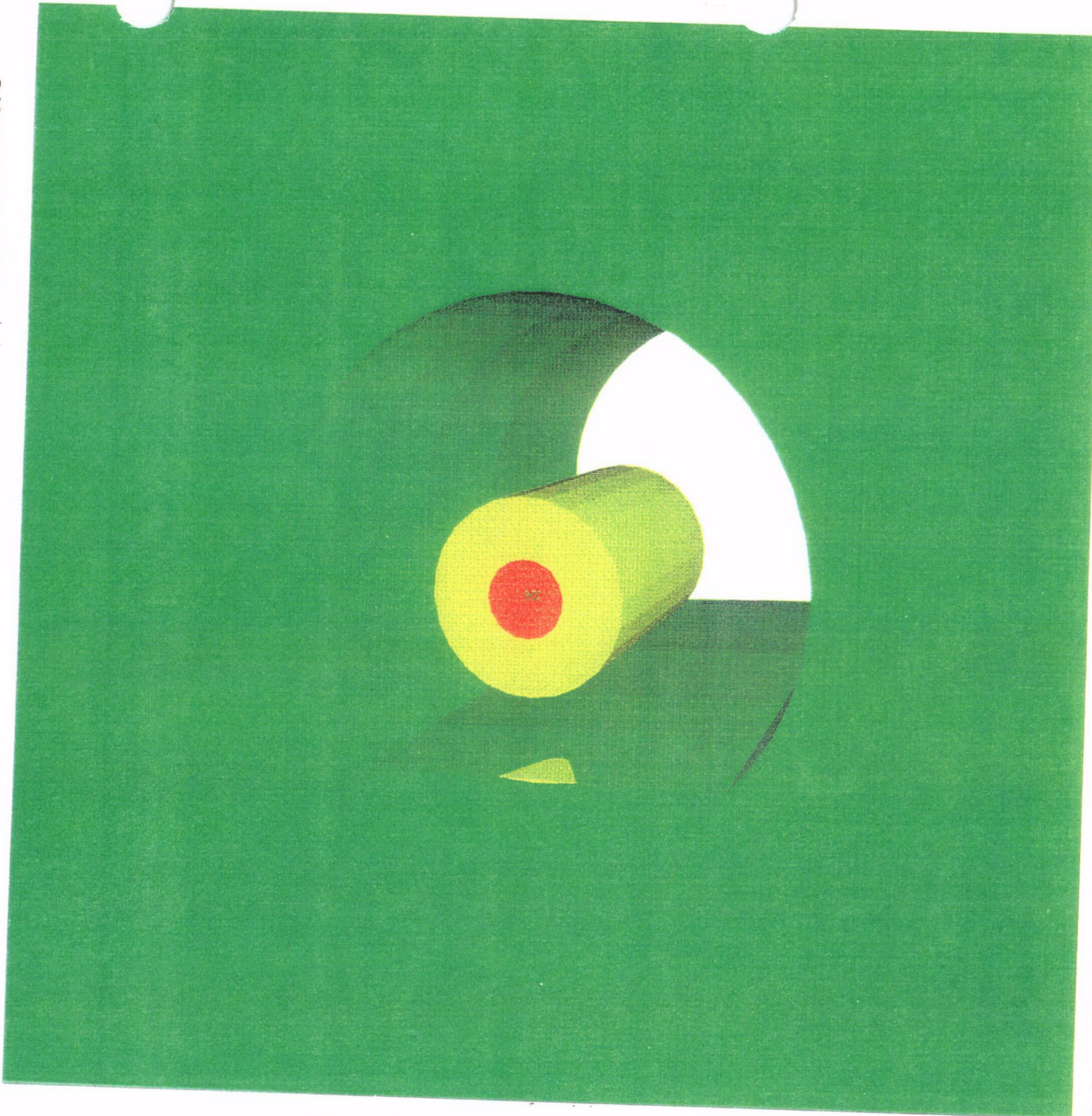
Figure 6.2-13. Low Thermal Load Emplacement Temperatures at 100 Years

ANSYS 5.0 A
JAN 25 1995

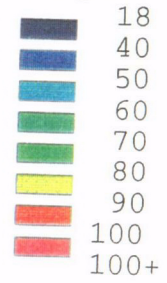
B00000000-01717-5705-00027 REV 00

6.2-29

March 1996



Temperature



Degrees C

21 PWR WP
Mid-plane
Temperatures

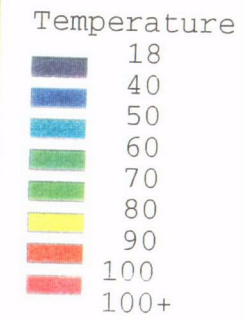
25 MTU/acre
(16.2 m WP Spacing)
(90 m Drift Spacing)

22 year old SNF
42.2 GWd/MTU

C17

Figure 6.2-14. Low Thermal Load Emplacement Temperatures at 500 Years

ANSYS 5.0 A
JAN 25 1995



21 PWR WP
Mid-plane
Temperatures

25 MTU/acre
(16.2 m WP Spacing)
(90 m Drift Spacing)

22 year old SNF
42.2 GWd/MTU

C18

Figure 6.2-15. Low Thermal Load Emplacement Temperatures at 1000 Years

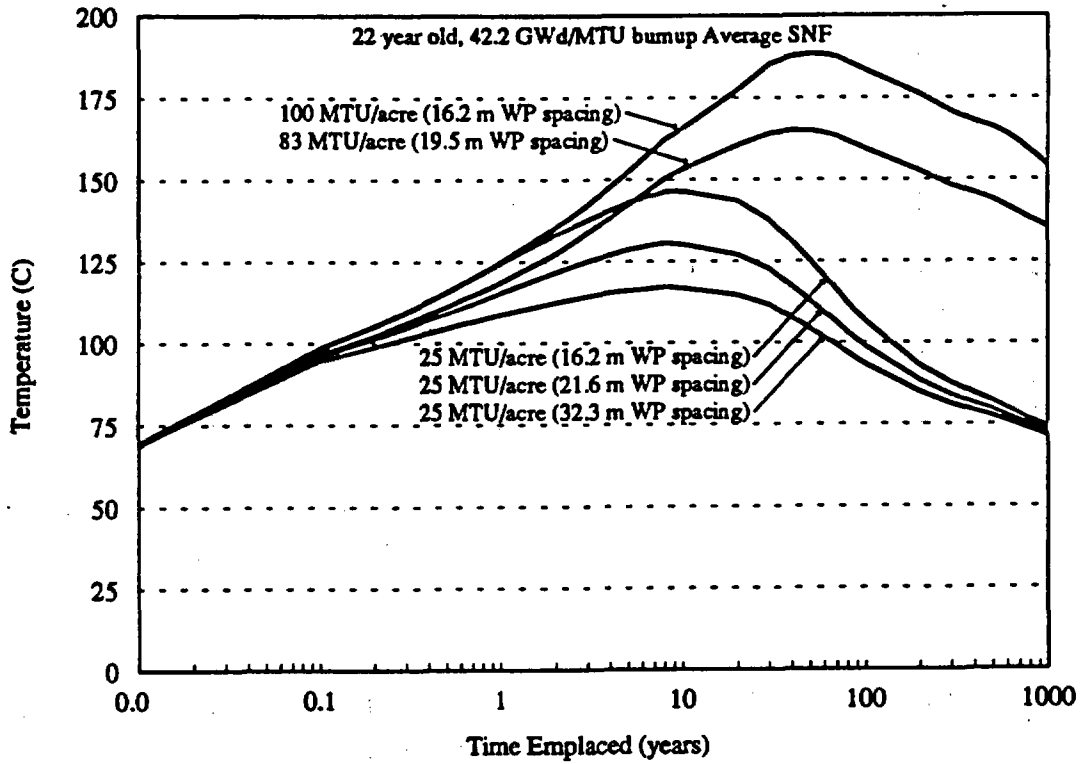


Figure 6.2-16. 21 PWR, WP Side Surface Temperatures

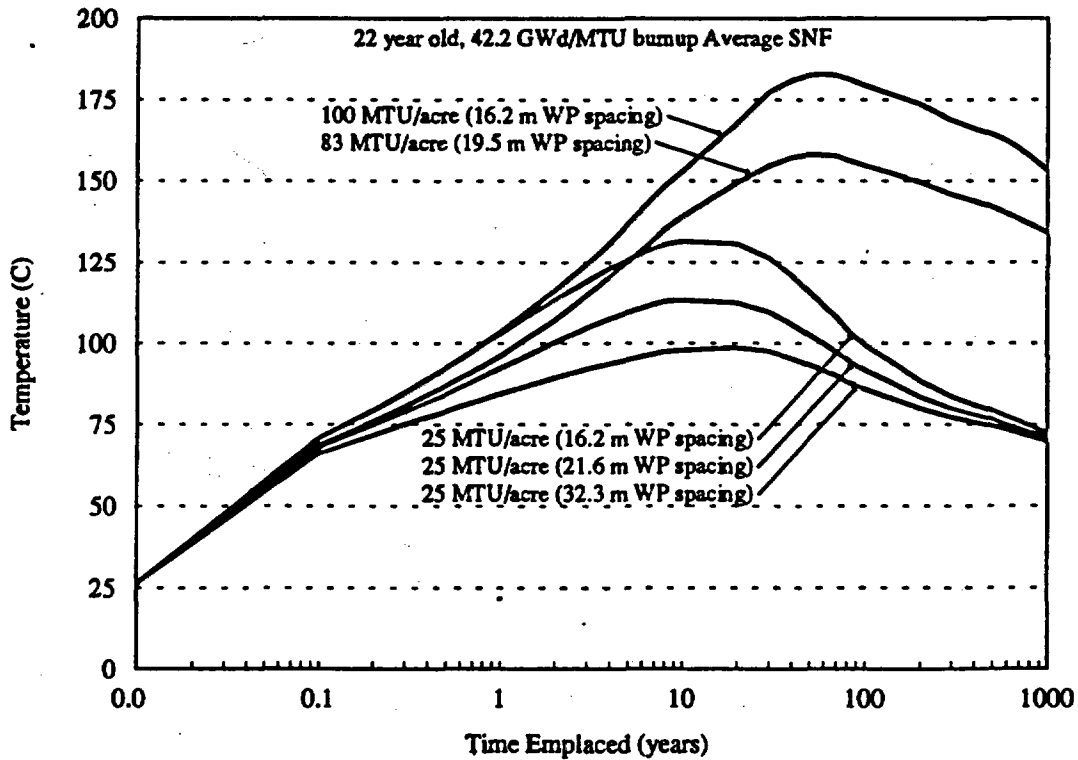


Figure 6.2-17. 21 PWR, Drift Side Wall Temperatures

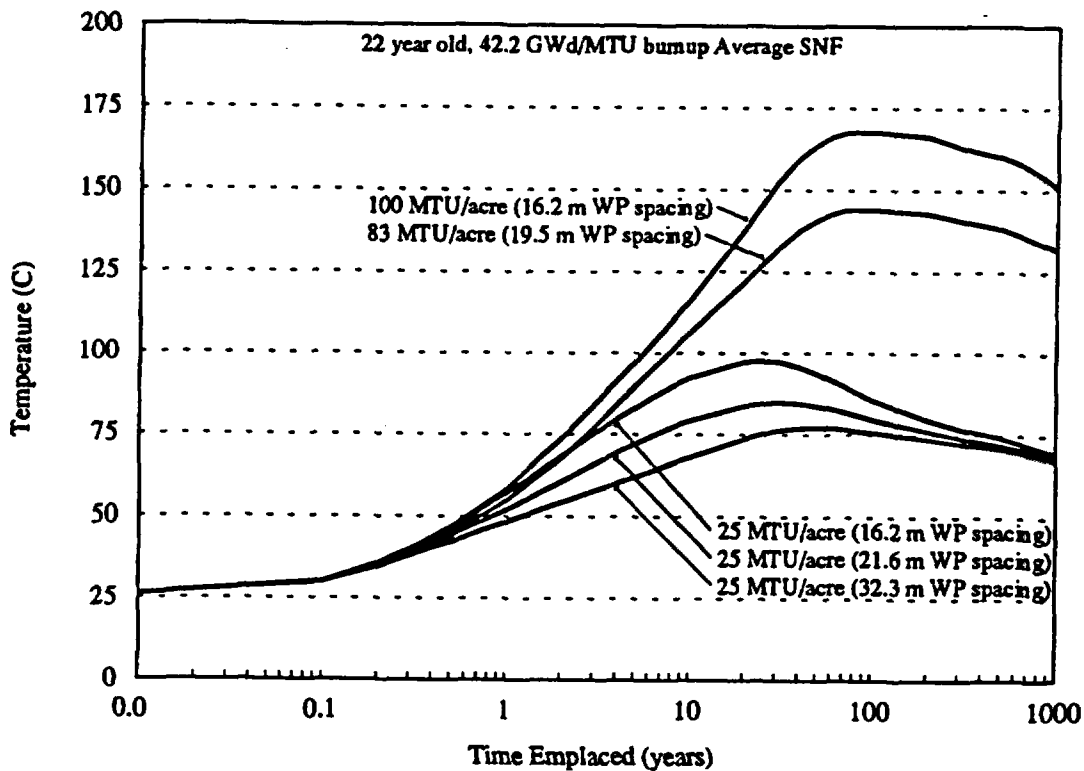


Figure 6.2-18. 21 PWR, 3 m from Drift Side Temperatures

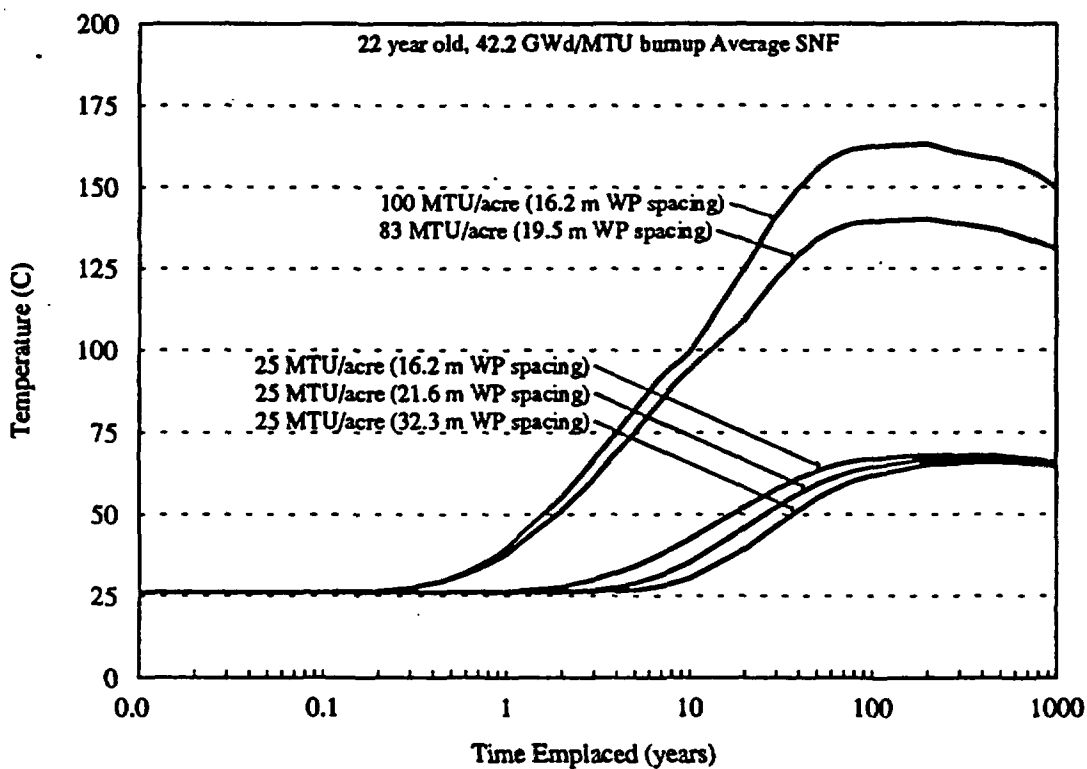


Figure 6.2-19. 21 PWR, Drift to Drift Midplane Temperatures

6.2.1.1.2 Small WPs: 12 PWR and 24 BWR

A range of thermal loadings was also evaluated to determine the near-field temperature effects of the small WP (12 PWR). The dimensions of the modeled WP were assumed to be those of the 12 PWR CF (assumed the conceptual MPC) with disposal container, which is representative of a smaller WP. The parametric set of thermal loading cases, summarized in Table 6.2-2, are similar to the cases described in Table 6.2-1. The 12 PWR packages are assumed emplaced with the same drift spacings as the 21 PWR packages with different WP spacings to achieve the same thermal loading. This is consistent with a repository that will contain both sizes of WPs. Again, representative "high" and "low" thermal loadings of 100 MTU/acre (24.7 kgU/m²), 83 MTU/acre (20.5 kgU/m²), and 25 MTU/acre (6.2 kgU/m²) were selected with drift spacings in multiples of 22.5 m. For all cases, the average SNF was 22 years old with 42.2 GWd/MTU burnup.

Table 6.2-2. 12 PWR Thermal Loading Scenarios

Areal Mass Loading MTU/acre	Initial Areal Power Density kW/acre	WP Spacing (m)	Drift Spacing (m)
100 (high #1)	113.7	9.2	22.5
83 (high #2)	94.4	11.1	22.5
25 (low #1)	28.4	18.5	45.0
25 (low #2)	28.4	12.3	67.5
25 (low #3)	28.4	9.2	90.0

The evaluation results indicate lower near-field temperatures for the 12 PWR WP compared to the 21 PWR WP; however, the temperatures at 3 m into the drift wall and beyond are virtually identical for the different WP capacities. The greatest difference between the 12 and 21 PWR WP surface temperatures was 21°C, and it occurred six months after emplacement for the low thermal loading #1 scenario. Figure 6.2-20 plots a comparison of maximum 12 PWR WP surface temperatures for the five thermal loading scenarios. Again, the shorter WP spacing of low thermal loading #3 resulted in higher near-field temperatures than high thermal loading #2 for the first five years. The long-term, near-field temperatures for the 12 PWR WP are the nearly the same as for the 21 PWR WP. Figure 6.2-21 compares the maximum drift wall temperatures for the five loadings, and Figure 6.2-22 compares the maximum temperature at 3 m into the drift wall. Maximum drift wall temperatures were no more than 16°C lower for the 12 PWR WP (compared to 21 PWR), and maximum 3 m rock temperatures were less than 3°C lower. Like the 21 PWR cases, the 12 PWR cases all had peak WP surface temperatures at or above the boiling point. Only low thermal loading #1 with the long WP spacing had maximum drift wall temperatures below boiling. Figure 6.2-23 compares the drift-to-drift midplane temperatures, which differed from the 21 PWR cases by less than 1°C.

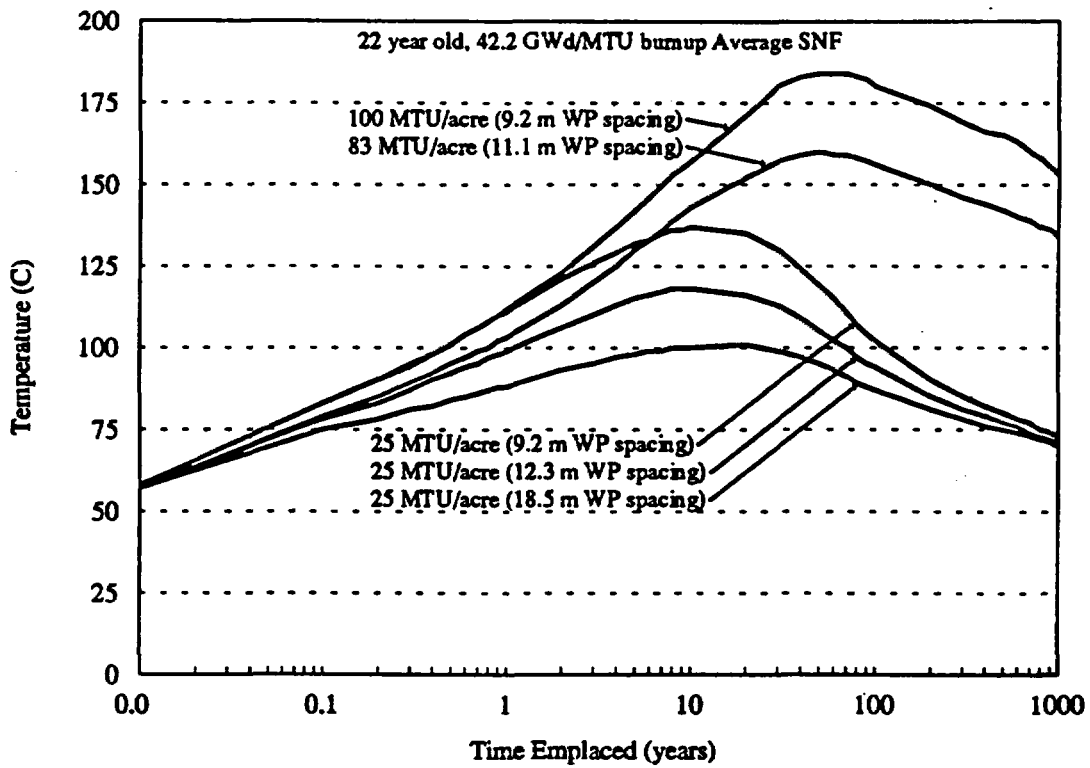


Figure 6.2-20. 12 PWR, WP Side Surface Temperatures

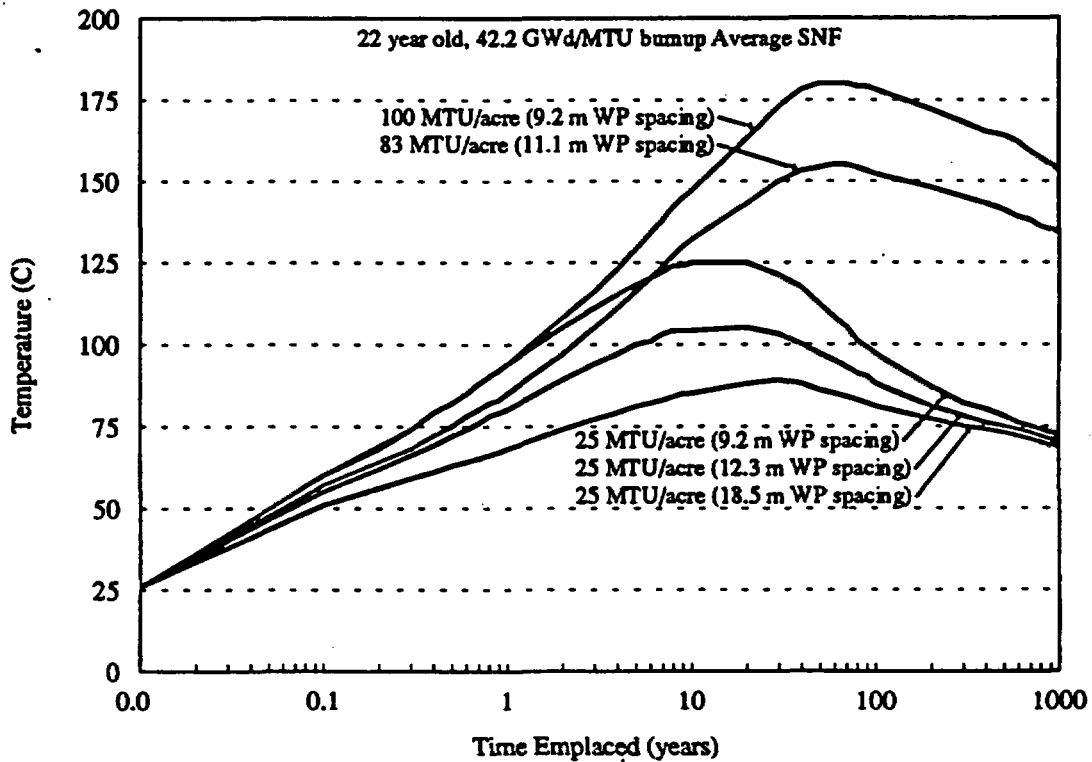


Figure 6.2-21. 12 PWR, Drift Side Wall Temperatures

The emplacement thermal evaluations for the 12 PWR WP provide the boundary conditions for more detailed evaluations of specific WP concepts. Like the 21 PWR emplacement model, the WP is represented by a homogeneous heat source such that the resulting near-field temperatures can represent any similar-capacity WP. For the purpose of the thermal evaluations in Sections 6.3 and 6.5, the surface temperatures predicted by the 12 PWR WP emplacement model can be assumed to apply to both the 12 PWR and the 24 BWR detailed thermal evaluations for CF and UCF WPs. Using PWR surface temperatures for the BWR analysis may be somewhat conservative as PWR package heat loads are generally greater than BWR heat loads.

6.2.1.1.3 Effect of Drift Backfill

A parametric analysis of the effect of backfilling the emplacement drift at repository closure was performed using the three-dimensional emplacement model described above. The base case without backfill was assumed to be the high thermal loading #1 of Table 6.2-1 for the 21 PWR WP. A thermal loading of 100 MTU/acre was chosen as the base for this parametric because it results in the highest (bounding) temperatures evaluated in Section 6.2.1.1.1.

The addition of a backfill material to the emplacement drift could be performed for any of several reasons. While it is a current program assumption (CRWMS M&O 1995n) that the drift will not be backfilled, a decision could be made at a later time that backfill is necessary to perform one of the following functions:

- Provide a capillary barrier to water contact with the WP.
- Reduce the relative humidity at the WP surface.
- Spread the flow of water or provide a drip shield.
- Provide a diffusion or retardation barrier against radionuclide release.
- Provide structural protection for the WP.
- Provide a chemical barrier (before water contacts the WP).

This parametric analysis evaluates the thermal impact of the addition of backfill material; however, it does not consider the "performance" of the backfill against any of the potential functions listed above. It is expected that the addition of backfill will insulate the WP such that WP temperatures increase. In an open emplacement drift, radiation heat transfer is the primary heat transfer path from the WP surface to the drift wall. If thermal radiation were replaced by an equivalent "imaginary" material, it would have an effective thermal conductivity of about 20 W/m·K (SNL 1993). This can be contrasted to concrete and TSw2 rock, which has thermal conductivities of 1.4 and 2.1 W/m·K, respectively. For crushed TSw2 tuff with a effective porosity of 0.48, estimates for effective thermal conductivity of 0.58 to 0.74 W/m·K have been reported (SNL 1995b).

Since it is not known what the backfill material will be (if any), a parametric was devised to determine what value of thermal conductivity is needed to maintain peak cladding temperatures below the cladding thermal goal (350°C). For the large WP, peak cladding temperatures generally occur within the first ten years (see Section 6.2.1.1.1). For the purpose of this evaluation, it was assumed that backfilling of the emplacement drifts is not performed until a repository closure time of 100 years after emplacement. To parametrically evaluate the response to backfill, the following range of backfill conductivities was considered: 0.2, 0.5, 0.6, 0.8, and 1.0 W/m·K.

Peak cladding and drift wall temperature results are displayed in Figures 6.2-24 and 6.2-25. Peak cladding temperatures are estimated based on predicted WP surface temperatures and a heat load dependent correlation (about 13°C/kW) derived from the detailed thermal evaluation of the 21 PWR CF with disposal container described in Section 6.5.1.1. As seen in Figure 6.2-24, a backfill conductivity of no less than 0.6 W/m·K is required to maintain cladding temperatures below 350°C when backfill is added at 100 years. If the backfill were added earlier after emplacement, a more conductive backfill would be needed. Backfill added at the time of emplacement would be much hotter than even borehole emplacement, because most backfill materials have conductivities lower than intact TSw2 rock. Borehole emplacement has been shown to be thermally incompatible with large WPs in previous evaluations (CRWMS M&O 1994i).

Figure 6.2-25 displays the temperature history of the emplacement drift wall adjacent to the WP with and without backfill. At the time of backfilling (100 years), drift wall temperatures drop because the backfill material is assumed to start at the ground surface average temperature of 18.7°C. However, temperatures quickly rise as the backfill absorbs heat from the WP and the drift wall. Drift wall temperatures near the WP actually increase after backfilling because the backfill prevents thermal radiation heat transfer, which would otherwise spread the WP heat over several meters of drift wall surface. Although drift wall temperatures increased, thermal goals for TSw2 rock were not exceeded. The magnitude of the second drift wall peak temperature after backfilling was not seen to depend on backfill conductivity.

6.2.1.1.4 Determination of Minimum WP Spacing

Two variations on WP spacing at 100 MTU/acre (high thermal loading #1) were considered to determine the impact of WP spacing on meeting near-field thermal goals. This parametric was devised to determine the smallest WP spacing achievable with the large WP (21 PWR) without violating thermal goals. In addition to high thermal loading #1 from Table 6.2-1, two additional cases were considered, which are summarized in Table 6.2-3. Drift spacings were modified for each case to maintain a thermal loading of 100 MTU/acre (24.7 kgU/m²).

Table 6.2-3. Minimum WP Spacing Thermal Loadings

Areal Mass Loading MTU/acre	Initial Areal Power Density kW/acre	WP Spacing (m)	Drift Spacing (m)
100 (high #1)	113.7	16.2	22.5
100 (high #3)	113.7	12.1	30.0
100 (high #4)	113.7	8.1	45.0

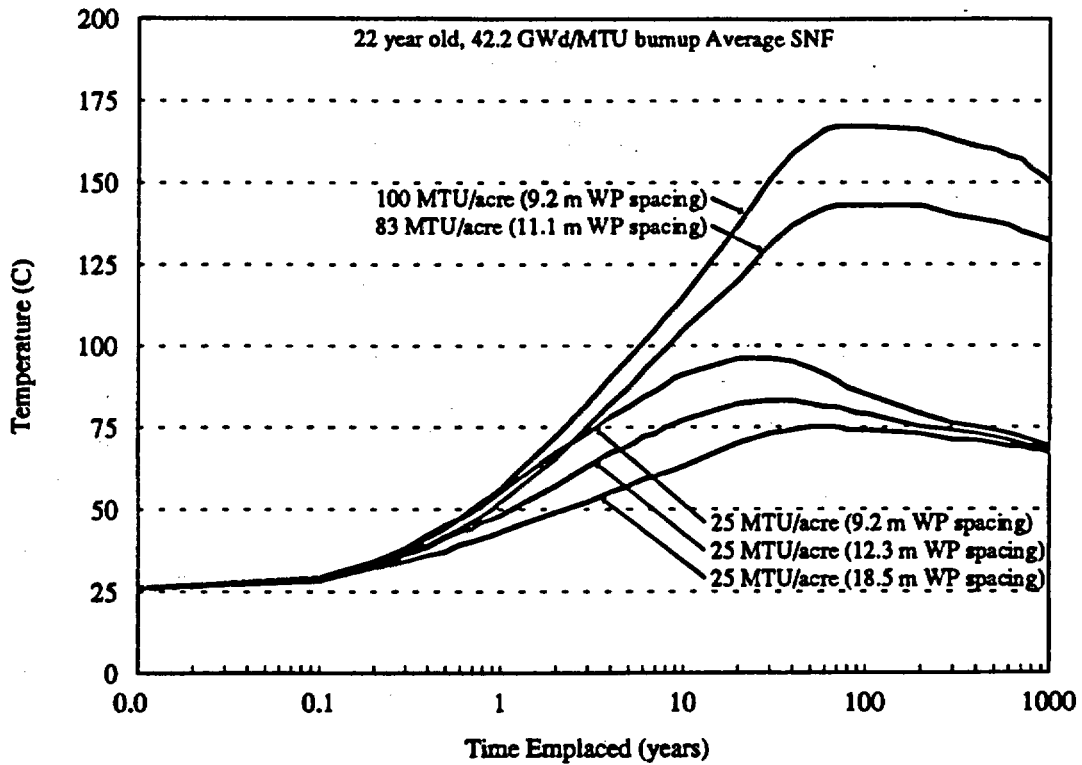


Figure 6.2-22. 12 PWR, 3 m from Drift Site Temperatures

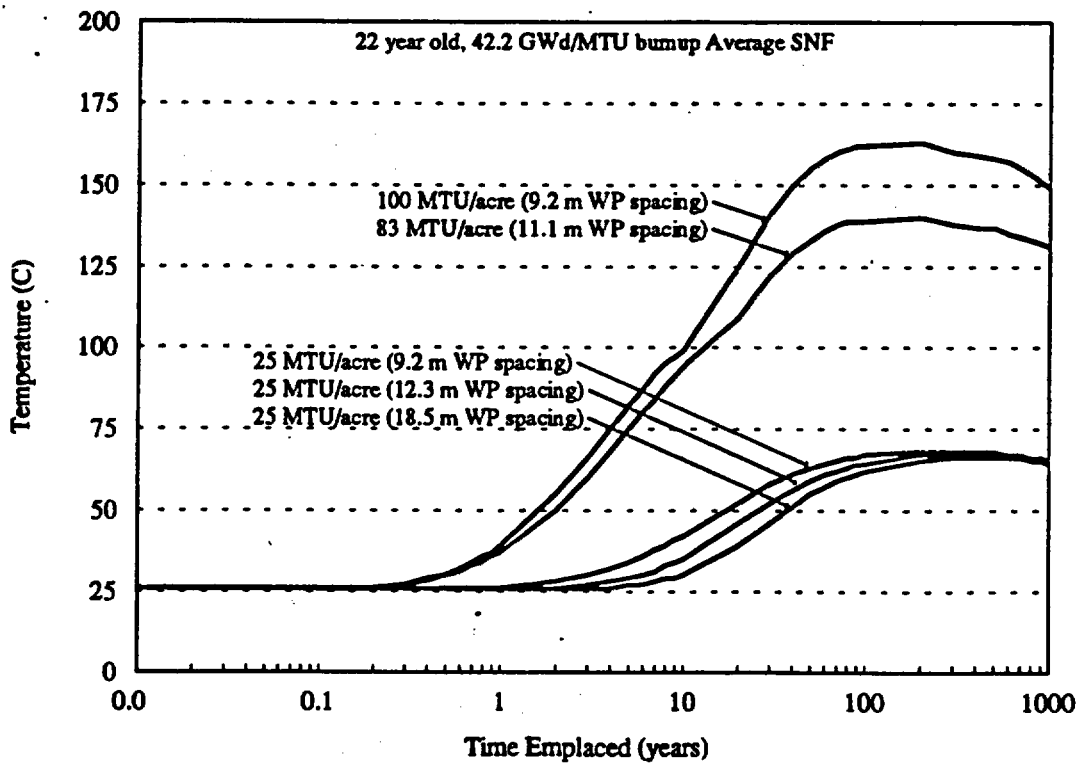


Figure 6.2-23. 12 PWR, Drift to Drift Midplane Temperatures

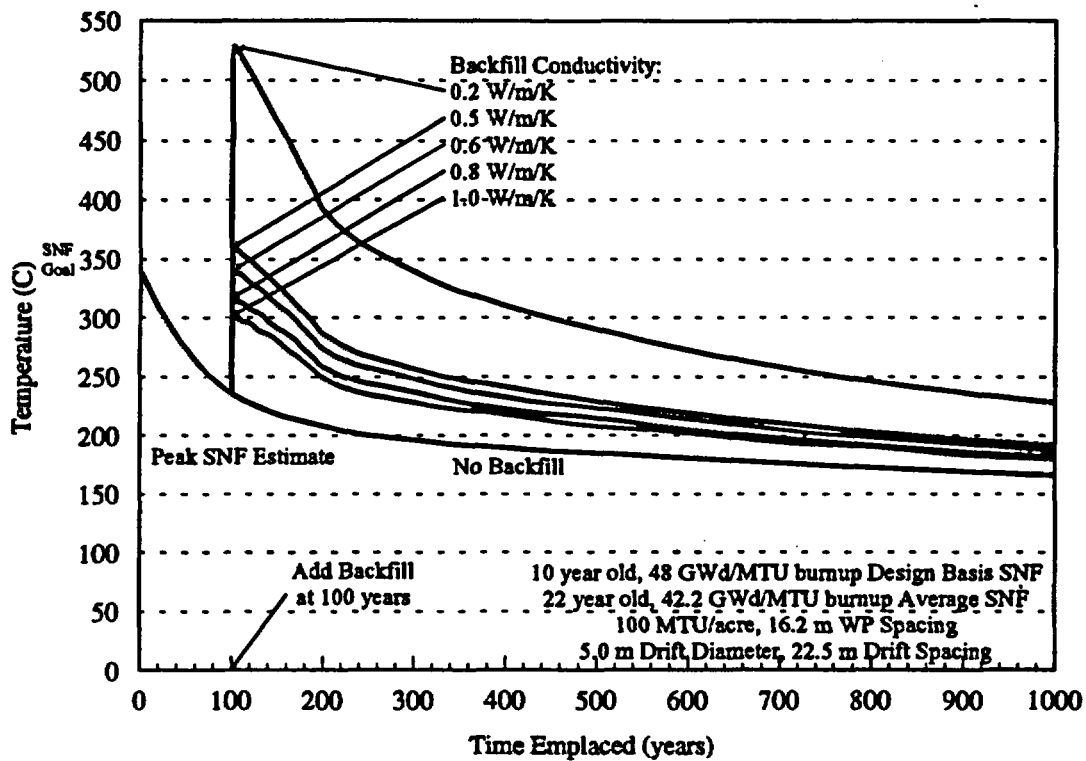


Figure 6.2-24. Effect of Drift Backfill on Cladding Temperature

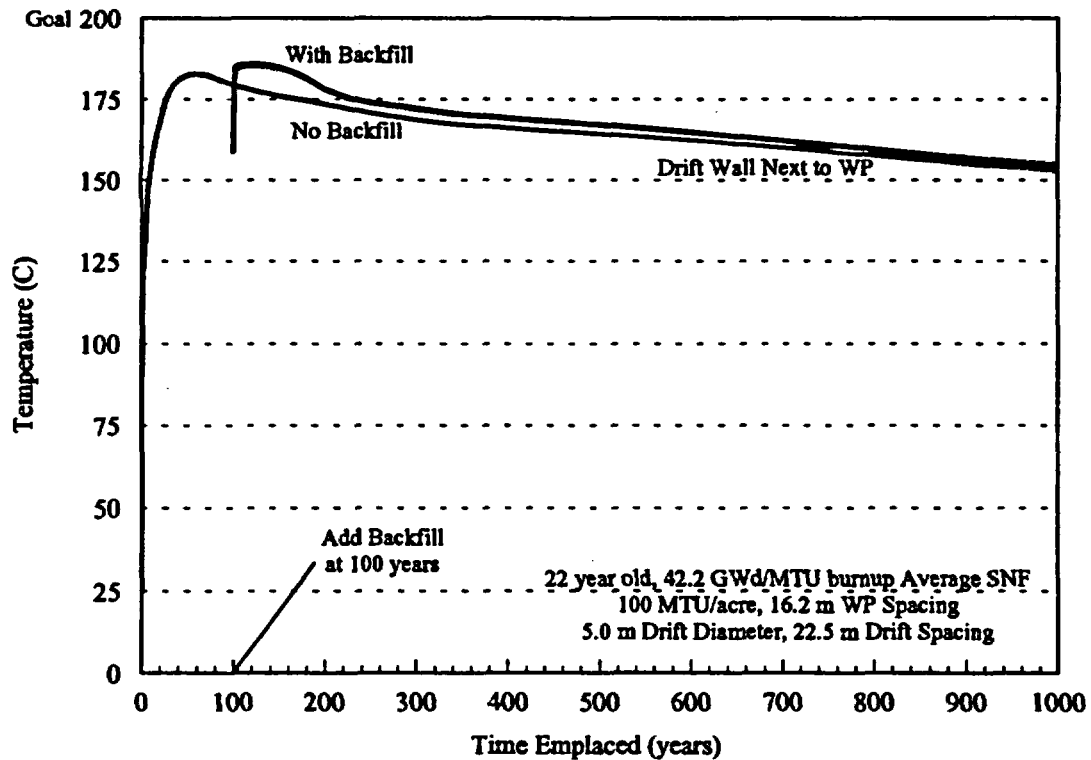


Figure 6.2-25. Effect of Drift Backfill on Drift Wall Temperature

In addition to the two above extra cases using the three-dimensional emplacement model (described in Section 6.2.1.1), the 21 PWR CF with disposal container detailed model (described in Section 6.5.1.1) was also rerun for these two cases to investigate the effect of shorter WP spacings on peak cladding temperatures. Both MGDS and MPC design basis SNF characteristics were considered and are reported in detail in a supporting design analysis (CRWMS M&O 1995d). Further description of the model and the high thermal loading #1 case for the 21 PWR CF is given in Figures 6.5-9 and 6.5-10, and in Section 6.5.1.1. A thermal loading of 100 MTU/acre was chosen as the base for this parametric because it results in the highest (bounding) temperatures evaluated in Section 6.2.1.1.1.

Figure 6.2-26 displays the effect of shorter WP spacings on peak cladding and drift wall temperatures. The results demonstrate that WP spacing is a key factor for near-field temperatures. Rock temperature thermal goals are clearly violated for the 8 m WP spacing with a peak drift wall temperature of 227°C (greater than 200°C drift wall temperature) and are near the limits with the 12 m WP spacing. Compared to the base 16 m WP spacing case, WP peak surface temperatures were 46°C hotter for the 8 m spacing and 10°C hotter for the 12 m spacing.

Peak cladding temperatures, estimated with the detailed CF model described in Section 6.5.1.1, were already close to the SNF cladding thermal goal (350°C) for the base 16 m WP spacing case. As seen in Figure 6.2-26, cladding temperatures are marginal with a 12 m spacing and exceed the cladding thermal goal with an 8 m spacing. Given a peak cladding temperature of 343°C and a peak drift wall temperature of 192°C for the 12 m WP spacing, WP spacings less than 12 m will likely exceed near-field thermal goals. And, given calculational and waste stream uncertainties (a WP with design basis SNF can generate 75 percent more heat than average), a minimum WP spacing of 16 m provides a conservative lower bound for large WPs such as the 21 PWR capacity CF with disposal container. This confirms previous scoping analysis, which made similar judgements.

6.2.1.1.5 WP Relocation

Relocation of WPs before repository closure has been suggested as a method for thermally managing WP heat loads that can vary significantly from one WP to the next. Conceptually, WPs could be repositioned in the emplacement drifts just before repository closure (assumed here to occur 100 years after emplacement) to adjust the areal power loading. In the *Waste Emplacement Management Evaluation Report* (CRWMS M&O 1995ah), it is suggested that the WPs could be relocated from 100 MTU/acre to 200 MTU/acre at 100 years to take advantage of extended dry conditions while avoiding the temperatures peaks that would otherwise occur during the first 100 years with an areal mass loading of 200 MTU/acre. However, the report also mentions that it is possible that thermal goals may be violated at such a high areal mass loading.

To determine the impact of doubling the areal mass loading at 100 years after emplacement, a variation of high thermal loading #1 described in Table 6-3 was evaluated. In this evaluation, the same initial thermal loading is assumed, but at 100 years, the WP spacing is halved to effectively double the areal mass loading to 200 MTU/acre. Figure 6.2-27 contrasts the thermal behavior of the reference 100 MTU/acre case to the scenario where WP relocation doubles the areal mass loading. Because the relocation takes place after 100 years, the SNF has aged sufficiently to avoid a violation of SNF cladding thermal goals. However, the relocation does result in TSw2 rock temperatures

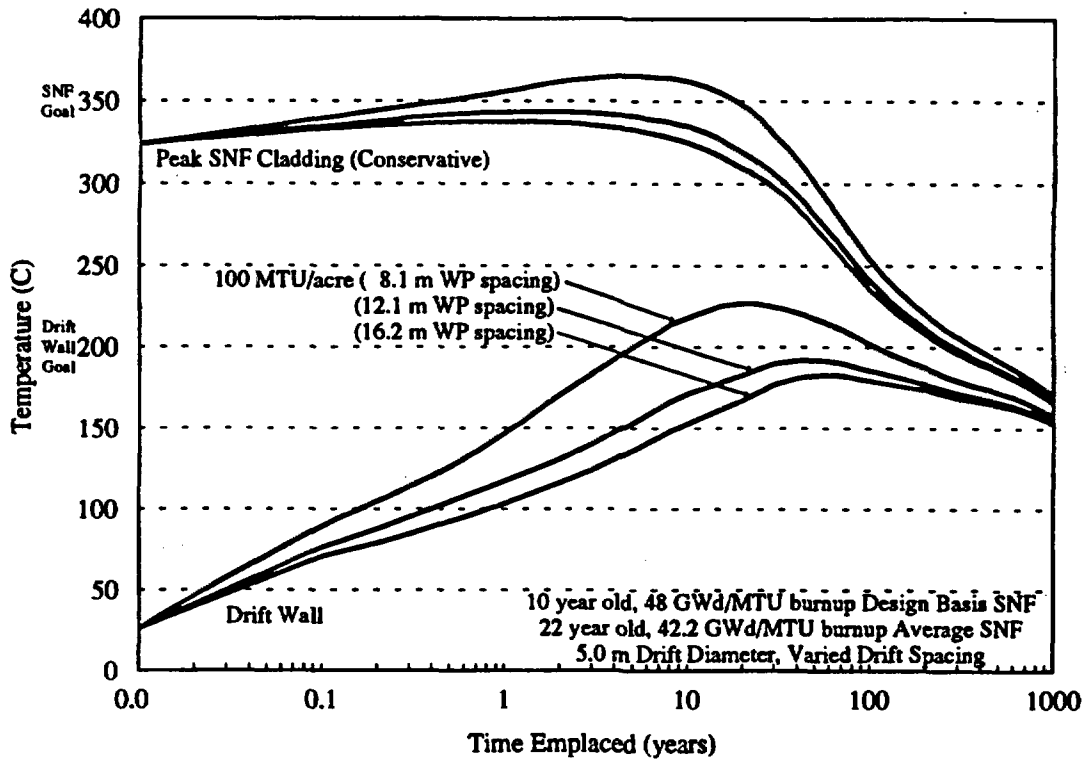


Figure 6.2-26. Temperatures used to Determine Minimum WP Spacing

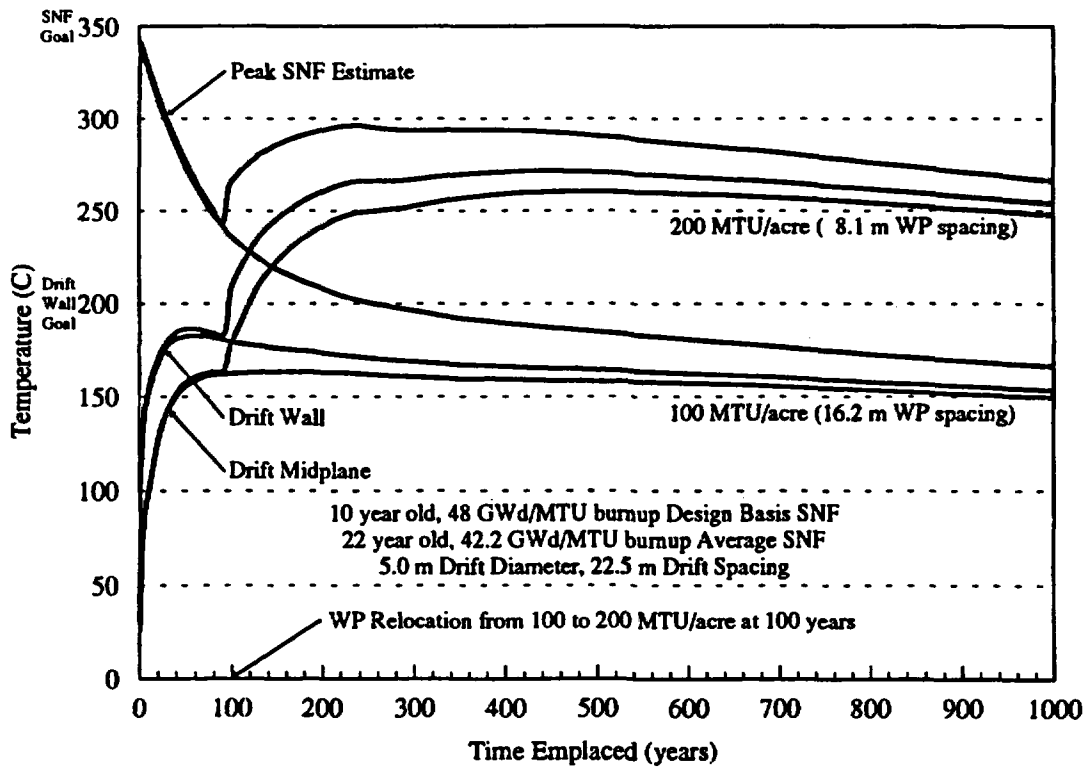


Figure 6.2-27. Effect of WP Relocation on Key Temperatures

much higher than the thermal goal of 200°C. Not only do maximum drift wall temperatures exceed the thermal goal, but average repository horizon temperatures exceed 250°C for more than 600 years. Also, the TSw3 rock layer reaches 179°C by 1,000 years, which is much above the thermal goal of 115°C.

The results of this evaluation clearly indicate that WP relocation resulting in areal mass loadings much above the maximum recommended by the FY 1993 *Thermal Loading System Study* (CRWMS M&O 1994h) will result in a violation of thermal goals. Thermal management techniques (such as WP relocation, aging, and ventilation) can be used to moderate temperatures during repository preclosure. However, the resulting areal mass loading will be the primary determination of long-term repository temperatures which affects engineered barrier corrosion mechanisms and rates and the ability of the host rock to impede the migration of radionuclides.

The analysis methodology used to investigate WP relocation can also be applied to other analyses of near-field temperatures. In the relocation analysis, two WPs in the emplacement drift were modeled— one producing heat at emplacement, and the other producing heat only after 100 years (to represent a halving of WP spacing at 100 years). With two modeled WPs, instead of just one assumed average WP, evaluations can be performed with two WPs with dissimilar heat loads. Future work in determining near-field emplacement temperatures will investigate the temperature difference between differently loaded WPs in the emplacement drift. It is expected that a WP loaded with design basis SNF will result in hotter near-field temperatures in the surrounding rock than is predicted by the previous model using only average SNF characteristics. Results of these evaluations will be presented in future reports.

6.2.1.1.6 Thermal Controlled Corrosion Regimes

Figure 6.2-28 plots WP surface temperatures for three thermal loadings with a 21 PWR WP in a 4.3-m (14-ft) drift and equal WP and drift spacings. There is concern over large WPs in a low thermal load (sometimes inappropriately referred to as "cold") repository due to possible aggressive corrosion at the WP surface. While there are insufficient test results to make a quantitative judgment of the corrosion impact, there is considerable evidence that aqueous corrosion is significantly more aggressive at temperatures between 60 and 100°C (see Aggressive Zone on Figure 6.2-28). This would primarily affect low thermal loadings where the WP surface is in the aggressive corrosion temperature range shortly after repository closure, and there may be inadequate rock dry out to prevent relative humidity from exceeding 60 to 70 percent (the threshold for aqueous corrosion). For the low thermal loading case, many or most WPs will experience this potentially aggressive corrosion environment during the first 1000 years after emplacement, a time period crucial to attaining containment performance objectives. The high thermal loading case will delay onset of this environment until well beyond the containment period, and the temperatures may fall below the aggressive range before the relative humidity can reach the threshold for aqueous corrosion. In addition, preliminary calculations by T. Buscheck of Lawrence Livermore National Laboratory (LLNL 1994a; LLNL 1994b) indicate that the higher thermal loadings yield significantly drier conditions throughout the repository than the low thermal loadings. To achieve cool surface temperatures with large WPs at low thermal loadings, the WPs can be spaced far apart and the SNF can be aged before emplacement. However, for the 21 PWR package, SNF ages of up to 100 years could be required to escape the aggressive zone for low thermal loads.

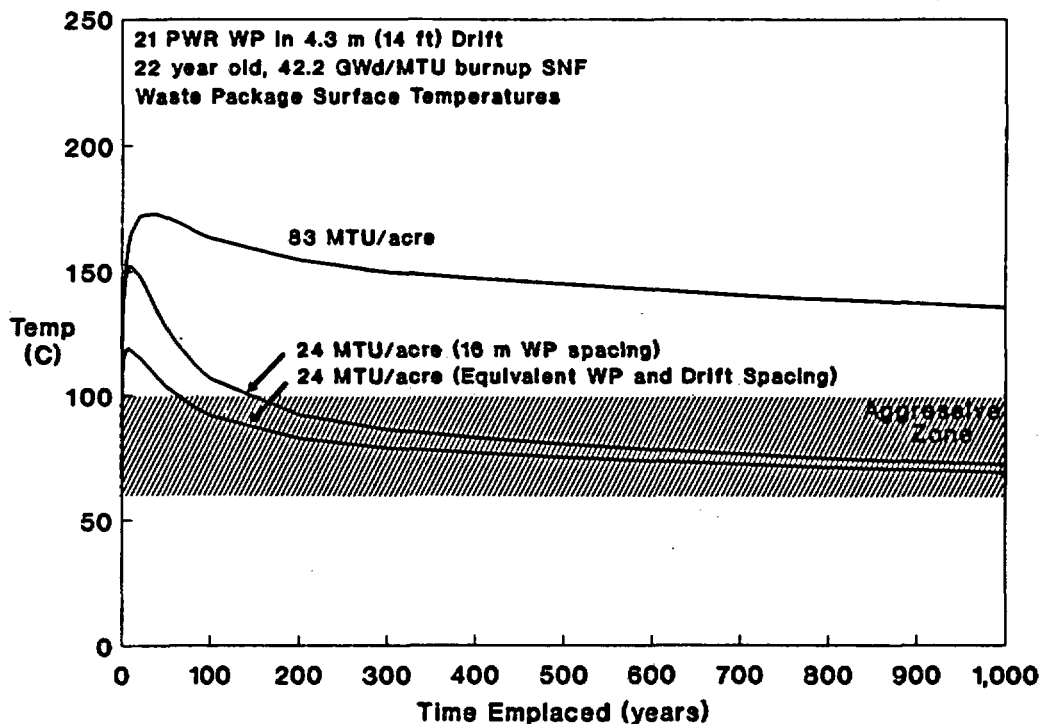


Figure 6.2-28. Potential for Aqueous Corrosion

There is also concern that, at temperatures below the boiling point and at relative humidities above 70 percent, microorganisms are potentially active, which could initiate microbiologically influenced corrosion. Figure 6.2-29 displays the microbiologically influenced corrosion active zones compared to WP surface temperature histories similar to those provided in Figure 6.2-28. A significantly more costly disposal container may be required for the large WPs at low thermal loads to withstand microbiologically influenced corrosion. If aging of the SNF is not possible or practical, a relatively more costly disposal container (compared with the two-barrier reference) could be developed to withstand the aggressive environment of aqueous corrosion and microbiologically influenced corrosion at low thermal loadings.

6.2.1.1.7 Aging of SNF Fuel in WPs

An analysis was conducted to determine the thermal effects of aging the SNF before emplacement with a 21 PWR capacity WP. Aging of SNF is of concern for thermal corrosion issues, as discussed in Section 6.1.1.1. The SNF age required to achieve a certain temperature will depend on the thermal loading selected as a reference. The reference case for the following analysis is the 24 MTU/acre square spacing (WP spacing = drift spacing = 38.9 meters) evaluation. The square spacing represents the largest practical WP spacing and will result in the lowest near-field temperatures for a given area mass loading.

Four SNF ages were considered for the parametric analysis: 22, 40, 80, and 100 years. Since the spacings and the SNF mass (assumed to be 0.428 MTU/assembly) were held constant, the area mass loading is the same for each case. However, the initial WP heat decreases with age and thus the initial areal power density decreases with SNF age. Note that for each evaluation, this model assumes every WP in the repository has the same heat output.

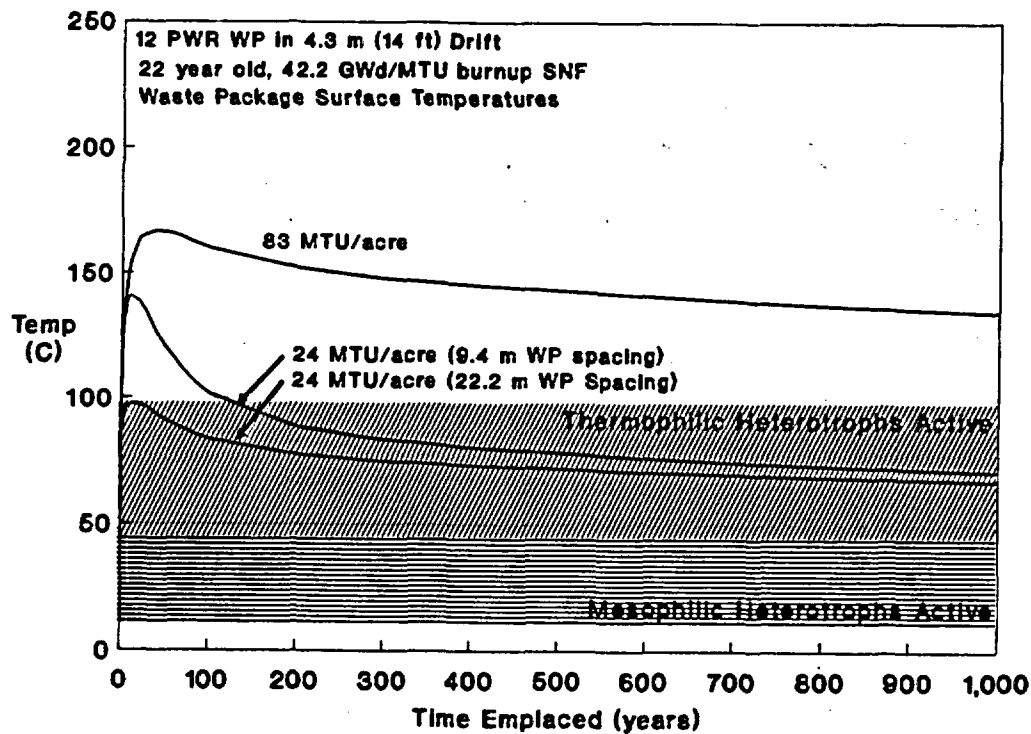


Figure 6.2-29. Microbiologically Influenced Corrosion

Table 6.2-4 summarizes the peak temperatures attained for each of the four SNF ages. The time of peak temperatures ranged from 7 years (for 22 year old SNF) to 500 years (for 100-year-old SNF). Figure 6.2-30 displays the WP surface temperature response to each SNF age. While each case has different short-term temperatures, long-term temperatures converge because all four cases have the same area mass loading.

Table 6.2-4. Peak Temperatures

	22-year-old SNF	40-year-old SNF	80-year-old SNF	100-year-old SNF
WP Side Surface	119°C	99°C	73°C	67°C
Maximum Drift Wall	100°C	83°C	64°C	61°C

Figure 6.2-30 indicates that an SNF aging of 40 years is required (at this area mass loading) to maintain WP surface temperatures below 100°C. However, more important from a corrosion standpoint, surface temperatures should be maintained below 60°C. With SNF aging of 100 years, the 21 PWR WP surface temperature reaches 67°C. If aging the SNF over 100 years is considered too costly and not practical, then a relatively more costly disposal container, such as a titanium alloy third barrier or a ceramic barrier, may need to be used to withstand the aggressive environment for aqueous corrosion and microbiologically influenced corrosion at low thermal loadings.

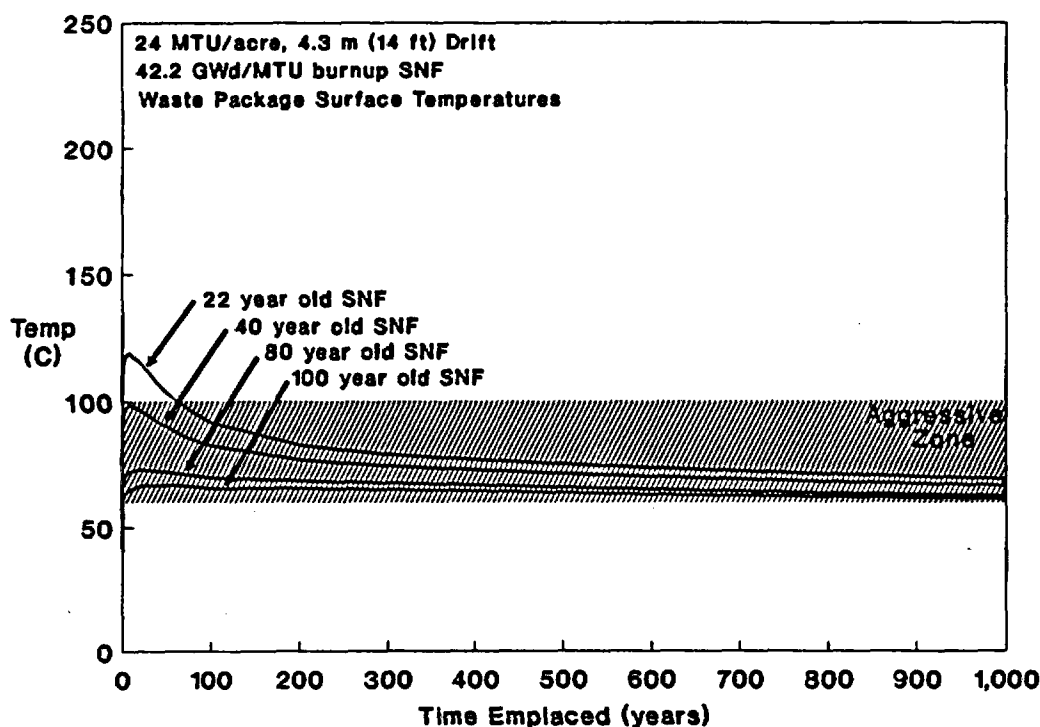


Figure 6.2-30. Aging of 21 PWR WP

6.2.1.2 SNF Thermal Response

The purpose of this section is to describe the development and application of the finite element model that predicts peak SNF temperatures for PWR assemblies. The SNF model is used to develop a basis for determining an effective thermal conductivity for an assembly with smeared/homogenous properties and to investigate the thermal behavior of an SNF assembly. The effective thermal conductivities developed here were used to predict peak cladding temperatures in the WP thermal evaluations in Sections 6.3 (UCF WP) and 6.5 (CF WP). While the effective thermal conductivity was originally developed for the thermal analysis of conceptual WP designs emplaced in the potential repository at Yucca Mountain, the methodology can be applied to storage and transportation thermal analyses as well.

For SNF, the Commercial Spent Fuel Management Program at Pacific Northwest Laboratory recommended a 380°C temperature limit (PNL 1983a) for the cladding to prevent creep rupture failure. A more conservative value of 350°C has been selected (CRWMS M&O 1993i) to account for uncertainties in source characteristics as well as heat transfer calculations. Over-prediction of SNF cladding temperatures in a thermal analysis can constrain the WP design and limit the capacity of potential WP concepts. Therefore, the following discussion addresses conservatism present in the different methods for predicting peak cladding temperatures.

6.2.1.2.1 Predicting Peak Cladding Temperatures

There are three methods available to estimate cladding temperatures inside a storage, transportation, or disposal device (cask, canister, or container). The first and most involved method is to explicitly model the canister and every fuel rod in every assembly within it. This model would directly consider the internal fill gas convection and conduction and a matrix of radiation view factors between the rods. A fluid-flow-capable computer code, such as FIDAP or COBRA-SFS, could be used to perform such an evaluation. This method is costly in setup and computational time and does not lend itself to parametric evaluation where detail is desired in the basket structure, corrosion barriers, and near-field rock, and not in an individual assembly.

The second method employs the Wooton-Epstein correlation (Wooton-Epstein 1963) to estimate the peak clad temperature based on the highest steady state temperature in the SNF basket structure. The Wooton-Epstein correlation has historically been the primary tool of transportation/storage cask vendors as it simplifies the analysis and has been previously accepted by the Nuclear Regulatory Commission. Thermal analyses of the CF conceptual design (CRWMS M&O 1994k) (for storage and transportation) and the BR-100 SNF shipping cask (BWFC 1991) used HEATING and PATRAN-P/THERMAL, respectively, to calculate SNF basket temperatures, which are the input to Wooton-Epstein. In these models, the SNF assemblies are modeled only as an edge heat flux to the basket structure without internal heat generation. The Wooton-Epstein relation then generates the estimated maximum steady state SNF cladding temperature. This method is not suited for WP evaluations as it requires multiple calculations, does not address transient behavior of the SNF and basket, does not predict the effects of differential loading of the canister, and may adversely affect basket profiles by forcing constant SNF assembly surface heat flux rates.

The third method of estimating peak clad temperatures is to prepare a finite element or finite difference model of the SNF assembly volume as a smeared solid with internal volumetric heat generation as part of the entire disposal container model. Instead of explicitly modeling the SNF rods, smeared properties for a homogenous assembly are assumed in the container model that will estimate the radiation and gaseous transport of heat from the assembly rods to the basket structure. An effective conductivity for the assembly volume can be defined that will simulate the temperature drop across a PWR assembly. If the effective conductivity is chosen carefully, the finite-element model will predict peak temperatures in the smeared-property assembly volume that are close to actual expected temperatures. This method has been used in the designs of the GA-4 (General Atomics 1993a) and GA-9 (General Atomics 1993b) truck casks and by the national laboratories, which have been tasked by the Nuclear Regulatory Commission to verify vendor calculations for the GA-4, BR-100, and other storage and transportation casks. The effective conductivity method can predict cladding temperatures with reasonable accuracy and allows the determination of transient behavior that will be experienced with repository emplacement.

The key to accurate SNF cladding temperature predictions using the effective conductivity method lies in determining the proper conductivity to assume in the assembly volume. The Wooton-Epstein correlation demonstrates that peak cladding temperatures are a function of the assembly type, the assembly decay heat, and the SNF basket wall temperature. It is important to note that the SNF basket wall temperature not only specifies the environment (edge) temperature for the assembly, but it also determines what portion of the decay heat will be transferred by thermal radiation. For an

SNF assembly in a gaseous environment, such as the helium fill gas assumed in the CF container, heat will be transferred by gaseous conduction, convection, and radiation. This temperature dependence for radiation heat transfer introduces severe nonlinearities into the calculation. Therefore, any effective conductivity will be highly temperature-dependent and cannot be specified by just one value for a given assembly type.

Due to the limitation of the first two methods, the effective conductivity method was employed for the parametric thermal evaluation of the CF container and the multibarrier WP (UCF) conceptual designs for emplacement in the potential geologic repository at Yucca Mountain. Previous thermal analyses of the CF (conceptual MPC) with disposal container in repository emplacement (CRWMS M&O 1993e; CRWMS M&O 1993g), performed in August 1993, assumed purposely conservative values for effective conductivity due to uncertainties in predicting SNF peak temperatures and in calculating effective conductivities. To determine the appropriate effective conductivity for a PWR assembly, a detailed two-dimensional model of a typical SNF assembly was developed using the ANSYS finite-element code including both gaseous heat transport and thermal radiation. After this model was run for a variety of SNF characteristics and temperature levels, a temperature and heat-load dependent effective conductivity for the homogeneous assembly was derived.

6.2.1.2.2 SNF Thermal Model

The B&W 15x15 Mark B4 PWR assembly (DOE 1992b) was chosen as the basis for the two-dimensional model, which, using symmetry, represents one-quarter of an assembly. Assuming two planes of symmetry, the model includes the basket wall, 45 full fuel rods, 14 half fuel rods, four guide tubes, and one-quarter of the center instrument tube.

Model detail included a 2 mil thick oxidation layer on the zircaloy 4 cladding (typical of fuel that has been in a reactor), and a gaseous (assumed helium) gap between the uranium oxide pellet and the cladding. The model assumes a uniform heat generation in the uranium pellets neglecting distributed radiation energy deposition in the cladding and supporting structures. In the future, investigation of volumetric radiation energy distribution within the assembly will be conducted as this distribution may have an impact on peak cladding temperatures. The two-dimensional WP thermal models described in Sections 6.3.3 and 6.5.1 do, however, assume an axial heat peaking factor to approximate the axial power distribution in a SNF assembly. Therefore, the volumetric assembly heat, calculated from the total SNF assembly heat production, is multiplied by an assembly heat peaking factor.

Helium (see Section 8.2.3) conduction and thermal radiation were assumed to transfer heat between the rods. Helium has poor buoyancy compared to its thermal conductivity (unlike air for example), and thus, helium convection heat transfer can be neglected compared to helium conduction in a horizontal assembly. Results of this model representing a horizontal assembly with helium fill gas can also be extrapolated to vertical configurations. Figure 4-18 of the *TN-24P PWR Spent-Fuel Storage Cask: Testing and Analyses* (PNL 1987c) demonstrates that axial convection with helium in a vertical cask is minimal. Axial temperature profiles were largely insensitive to cask orientation with helium compared to nitrogen, which exhibited significant axial heat transfer due to convection. The similarity between the peak temperatures in the horizontal and vertical helium tests was

attributed to the enhanced conduction heat transfer resulting from SNF assemblies contacting the basket in the horizontal orientation compensating for the loss of convection of helium.

Radiation heat transfer introduces a nonlinear effect to the thermal analysis. Superposition cannot be applied due to the nonlinearities and the model must be evaluated at a variety of temperature levels. The boundary temperatures will range from the highest SNF basket temperatures expected (when the emplaced WP internal temperatures peak) to ambient repository rock conditions (the coldest the WP could be). To model the radiation heat transfer, a matrix of radiation view-factors was explicitly generated for each element face by the ANSYS code.

Material properties for the assembly model were taken from the *MATPRO Handbook* (EG&G 1981) and include temperature-dependent conductivities and oxidation-dependent emissivities (about 0.8). However, other effects such as fuel densification, swelling, restructuring, cladding dimensional changes (creepdown, thermal expansion, elastic deformation, stress irradiation growth), and fission product gas release were neglected as they have only a small effect on temperatures within the SNF cladding. A detailed description of model development assumptions and dimensions are provided in a supporting design analysis (CRWMS M&O 1995ai).

Design-basis SNF characteristics vary for storage, transportation, and disposal thermal evaluations. A matrix of different characteristics was assumed for this analysis to encompass as much of the fuel that could be loaded into the WP as possible. For a steady-state evaluation, different SNF characteristics translate to different steady-state volumetric heat loads. The model was evaluated over a range of heat generations—from the oldest and coolest fuel, to the youngest and hottest.

6.2.1.2.3 Matrix of Solution Cases

Assuming the B&W assembly type and helium fill gas, a matrix of SNF model solution cases was developed. The results of these cases are used to determine the temperature and heat load dependence of the calculated effective conductivities. To bound the possible operational range of SNF environments for repository disposal, nine basket temperatures were selected: 25, 50, 100, 150, 200, 250, 300, 350, and 400°C. This range is intended to cover possible WP temperatures from values greater than the SNF cladding limit of 350°C (CRWMS M&O 1993i) to potential repository ambient rock temperatures of about 25°C. Four SNF heat loads were also selected based on the various SNF types that could be received at the repository: 250, 500, 750, and 1000 W. For comparison, the 10-year-old, 40 GWd/MTU PWR SNF type assumed for the conceptual MPC analyses (CRWMS M&O 1993e) generates 676 W at emplacement, and an assumed repository average of 22 years old and 42.2 GWd/MTU burnup generates 487 W.

The peak cladding temperature predictions for each of the 36 SNF model cases are summarized in Table 6.2-5. As expected, the highest cladding temperatures occurred for the high basket temperature and high heat load case. Temperature profiles within the assembly were reasonable, as demonstrated in Figure 6.2-32, which displays temperature contours for the case with an assembly heat of 750 W and a basket wall temperature of 300°C. This case is the most similar to the conditions predicted in the thermal analysis of the MPC conceptual design with disposal container (CRWMS M&O 1993e).

Table 6.2-5. Peak Cladding Temperatures: SNF Assembly Model

Basket Wall Temperature	Assembly Heat Load			
	250 W	500 W	750 W	1000 W
25°C	38	51	63	74
50°C	62	74	85	96
100°C	110	120	129	139
150°C	159	167	175	183
200°C	207	214	221	228
250°C	256	262	268	274
300°C	305	311	316	321
350°C	355	359	364	368
400°C	404	408	412	416

Table 6.2-6. Cladding-to-Basket Delta T: SNF Assembly Model

Basket Wall Temperature	Assembly Heat Load			
	250 W	500 W	750 W	1000 W
25°C	13	26	38	49
50°C	12	24	35	46
100°C	10	20	29	39
150°C	9	17	25	33
200°C	7	14	21	28
250°C	6	12	18	24
300°C	5	11	16	21
350°C	5	9	14	18
400°C	4	8	12	16

The results in Table 6.2-5 are consistent with the test case results from preliminary calculations (CRWMS M&O 1994m) and demonstrate some of the expected trending. Table 6.2-6 illustrates this trending by summarizing the cladding-to-basket wall temperature drops (ΔT) for each case. Without the contribution of thermal radiation as a heat transfer mechanism, one might expect that the temperature drop would depend on the assembly heat load only (i.e., $q''=(k/L)\cdot\Delta T$). However, Table 6.2-6 shows that there is a nonlinear temperature dependence in the temperature drop, which would imply a nonlinear effective conductivity (k_e) (see Section 6.2.1.2.4).

Because the radiation heat transfer depends on T^4 , i.e., $q''=\epsilon\sigma(T_1^4-T_2^4)$, there is less thermal resistance as absolute temperatures increase and, therefore, the temperature drop decreases at higher temperatures. As expected, the temperature drop will increase with increasing heat load. The implication is that to define an effective conductivity, k_e , such that $q''=(k_e/L)\cdot\Delta T$, the effective conductivity must be temperature-dependent. Because of the multiple non-linearities involved in an SNF assembly thermal analysis, there may also be a heat load dependence on k_e as well. Section 6.2.1.2.4 investigates this trending in the determination of an effective conductivity.

To check the above SNF model preliminary results, the Wooton-Epstein correlation (Wooton-Epstein 1963) was applied for each of the cases. This empirically derived correlation was shown to be conservative in Section 3.6.2 of the *BR-100 Spent Fuel Shipping Cask Report* (BWFC 1991). For the Wooton-Epstein analysis, the same material properties and conditions assumed in the ANSYS SNF model were used. Table 6.2-7 summarizes the peak cladding results of the Wooton-Epstein calculation and Table 6.2-8 provides the calculated cladding-to-basket temperature drops (ΔT).

As expected, the Wooton-Epstein correlation was conservative, compared to the ANSYS SNF model, in all cases. Similar behavior is also observed for the cladding-to-basket temperature drop. The temperature drop (ΔT) decreased with increasing absolute temperature, and increased with assembly heat load. For each case, the ΔT was roughly twice that predicted by the ANSYS SNF model. This result is expected as the detail of the SNF model provides a "best estimate" of SNF cladding temperatures compared to the Wooton-Epstein correlation, which provides conservative temperature predictions over a certain range.

6.2.1.2.4 Determination of Effective Thermal Conductivity

In the conceptual MPC/WP thermal model (CRWMS M&O 1993e), the SNF assembly is represented by a solid square with smeared material properties. While the density and heat capacity can be calculated based on a weighted average of the materials present, the thermal conductivity of the SNF assembly area must take into account convection, conduction, and radiation heat transfer across the assembly. Some work to this effect has been done for consolidated assemblies; however, information is sketchy for intact assemblies. The final design report for the GA-4 truck cask (General Atomics 1993a) gives one relation for PWR SNF effective thermal conductivity. Evaluating the relation results in conductivities from 0.399 W/m·K at 0°C to 1.316 W/m·K at 400°C. For comparison, a consolidated assembly in a vacuum may have a smeared conductivity from 0.060 to 0.590 W/m·K (Westinghouse 1982) over the same range. These consolidated SNF values were used in several evaluations by Lawrence Livermore National Laboratory of consolidated SNF in borehole emplaced WPs (LLNL 1991a). An attempt made to calculate an effective medium

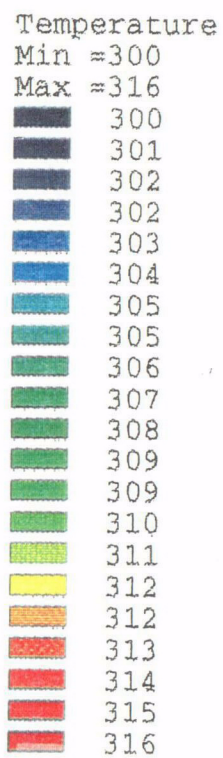
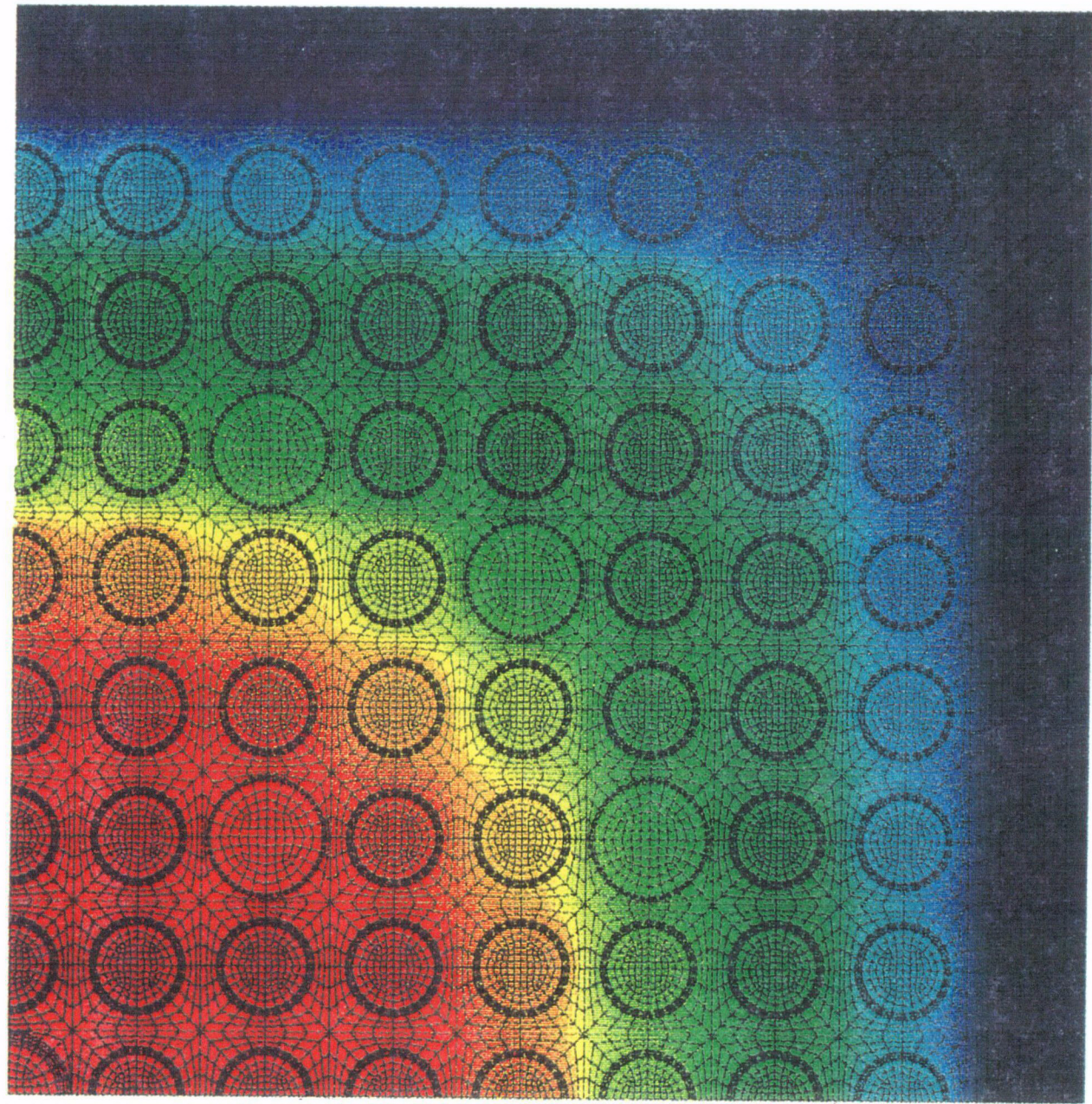
INTENTIONALLY LEFT BLANK

ANSYS 5.0 A
FEB 3 1995

B00000000-01717-5705-00027 REV 00 Vol. III

6.2-53

March 1996



Degrees C

750 Watts/assembly
300°C Basket Wall

Figure 6.2-31. SNF Assembly Model Temperatures

C19

Table 6.2-7. Peak Cladding Temperatures: Wooton-Epstein Correlation

Basket Wall Temperature	Assembly Heat Load			
	250 W	500 W	750 W	1000 W
25°C	52°C	71°C	88°C	103°C
50°C	76°C	94°C	111°C	125°C
100°C	123°C	140°C	155°C	168°C
150°C	170°C	185°C	199°C	211°C
200°C	217°C	231°C	243°C	254°C
250°C	265°C	277°C	288°C	298°C
300°C	312°C	323°C	332°C	341°C
350°C	360°C	369°C	378°C	386°C
400°C	409°C	416°C	424°C	431°C

Table 6.2-8. Cladding-to-Basket Delta T: Wooton-Epstein Correlation

Basket Wall Temperature	Assembly Heat Load			
	250 W	500 W	750 W	1000 W
25°C	27°C	46°C	63°C	78°C
50°C	26°C	44°C	61°C	75°C
100°C	23°C	40°C	55°C	68°C
150°C	20°C	35°C	49°C	61°C
200°C	17°C	31°C	43°C	54°C
250°C	15°C	27°C	38°C	48°C
300°C	12°C	23°C	32°C	41°C
350°C	10°C	19°C	28°C	36°C
400°C	9°C	16°C	24°C	31°C

conductivity using debris bed conductivity correlations (Cook and Peckover 1982) resulted in an estimate of 0.127 W/m·K. As observed in the previous sections, a single value for an effective conductivity is not sufficient due to the radiation induced nonlinearities present.

The purpose of the effective thermal conductivity is to relate the temperature drop of a homogeneous heat generating square to the temperature drop across an actual assembly. Given the heat load and temperature drop calculated with a discrete model of an SNF assembly, we wish to calculate here the effective conductivity of the homogenous heat-generating square. An analytical solution of the heat diffusion equation for a steady temperature in a rectangle with heat generation is given by Equation 5.5-6 in Carslaw and Jaeger (Carslaw and Jaeger 1959).

Assuming isotropic thermal conductivity and superposition, evaluating at the center of the square ($x=y=0$), and solving for an effective conductivity (k_e) results in Equation 6.2-1 (CRWMS M&O 1995ai):

$$k_e = \frac{Q}{4L_a(T_o - T_s)} (0.2947) \quad \text{(Equation 6.2-1)}$$

where:

- Q = Assembly heat generation (watts)
- L_a = Assembly active length (meters)
- T_o = Center temperature (peak cladding C)
- T_s = Surface temperature (basket wall C)

Equation 6.2-1 was used to predict an effective conductivity for each temperature and heat load used. The calculation was performed for both the ANSYS SNF model solutions from Table 6.2-5 and the Wooton-Epstein comparisons from Table 6.2-7. Tables 6.2-9 and 6.2-10 summarize the effective conductivity determination for the SNF model and Wooton-Epstein respectively. As expected, the effective conductivity is highly temperature-dependent; however, for the SNF model results, there was little dependence on the assembly heat load. This is contrasted to the Wooton-Epstein results where there was some dependence on heat load observed, though less evident than the temperature dependence.

Some thermal analysis codes are capable of solving with temperature-dependent material properties; however, very few can handle more than one dimension of nonlinearity in the properties. If the heat load dependence for the effective conductivity can be shown to be small, then a more useful conductivity can be defined that is a function of temperature only. As described earlier, this temperature-dependent conductivity could then be used to predict peak cladding temperatures in the cask or WP model, avoiding the extra calculation of empirical correlations.

Table 6.2-11 presents the averages over the heat loads from Tables 6.2-9 and 6.2-10 and compares them to effective conductivities from references for intact (General Atomics 1993a) and consolidated (Westinghouse 1982) SNF. Previous analyses of the conceptual MPC with disposal container (CRWMS M&O 1993e) used estimated effective conductivities that were even more conservative

Table 6.2-9. Effective Conductivity (W/m·K): SNF Assembly Model

Basket Wall Temperature	Assembly Heat Load			
	250 W	500 W	750 W	1000 W
25°C	0.45	0.46	0.47	0.48
50°C	0.49	0.50	0.51	0.52
100°C	0.58	0.59	0.60	0.61
150°C	0.69	0.70	0.71	0.72
200°C	0.82	0.82	0.83	0.84
250°C	0.96	0.97	0.97	0.98
300°C	1.12	1.13	1.14	1.14
350°C	1.30	1.30	1.31	1.32
400°C	1.49	1.50	1.51	1.52

Table 6.2-10. Effective Conductivity (W/m·K): Wooton-Epstein Correlation

Basket Wall Temperature	Assembly Heat Load			
	250 W	500 W	750 W	1000 W
25°C	0.22	0.25	0.28	0.30
50°C	0.23	0.27	0.29	0.31
100°C	0.26	0.30	0.32	0.35
150°C	0.30	0.33	0.36	0.38
200°C	0.34	0.38	0.41	0.43
250°C	0.41	0.44	0.47	0.50
300°C	0.48	0.52	0.55	0.57
350°C	0.57	0.61	0.64	0.66
400°C	0.68	0.72	0.75	0.77

Table 6.2-11. Comparison of Temperature-Dependent Effective Conductivities

Basket Wall Temperature	Average k_e SNF Model	Average k_e Wooton-Epstein	Intact PWR SNF k_e	Consolidated SNF k_e
25°C	0.462	0.263	0.431	0.065
50°C	0.504	0.275	0.466	0.070
100°C	0.597	0.305	0.544	0.093
150°C	0.705	0.344	0.634	0.135
200°C	0.829	0.393	0.737	0.190
250°C	0.970	0.454	0.855	0.263
300°C	1.130	0.530	0.990	0.355
350°C	1.307	0.620	1.143	0.460
400°C	1.504	0.728	1.316	0.590

than those predicted with the Wooton-Epstein correlation. Therefore, thermal analyses using the effective conductivities calculated from the SNF model would provide a "best estimate" of peak cladding temperatures compared to the conservative predictions derived from Wooton-Epstein or previous conservative effective conductivities.

Figure 6.2-32 provides a graphical comparison of the effective thermal conductivities of Table 6.2-11. The importance of radiation heat transfer in an array of heated rods is evident from the difference between consolidated and intact SNF. In the consolidated assembly, there is some contact between rods, which results in better conduction compared to convection and conduction across a fill gas in the intact assembly. However, the radiation heat transfer in the consolidated assembly is limited in range compared to the more sparse array of an intact assembly. For the elevated temperatures experienced by an SNF assembly, radiation heat transfer will play a dominant role.

The results in Figure 6.2-32 and above in Table 6.2-11 indicate varying degrees of conservatism in determining an effective conductivity. The Wooton-Epstein correlation provides a conservative (lower conductivity means higher temperatures) temperature estimation compared to best estimate predictions using the SNF model effective conductivities. Effective thermal conductivities derived from the SNF model compare quite well with effective conductivities developed by General Atomics for the GA-4 cask; the GA-4 values are found to be just slightly more conservative. For an intact PWR SNF assembly with helium fill gas, the conductivities derived from the SNF model should provide a best estimate of SNF cladding temperatures.

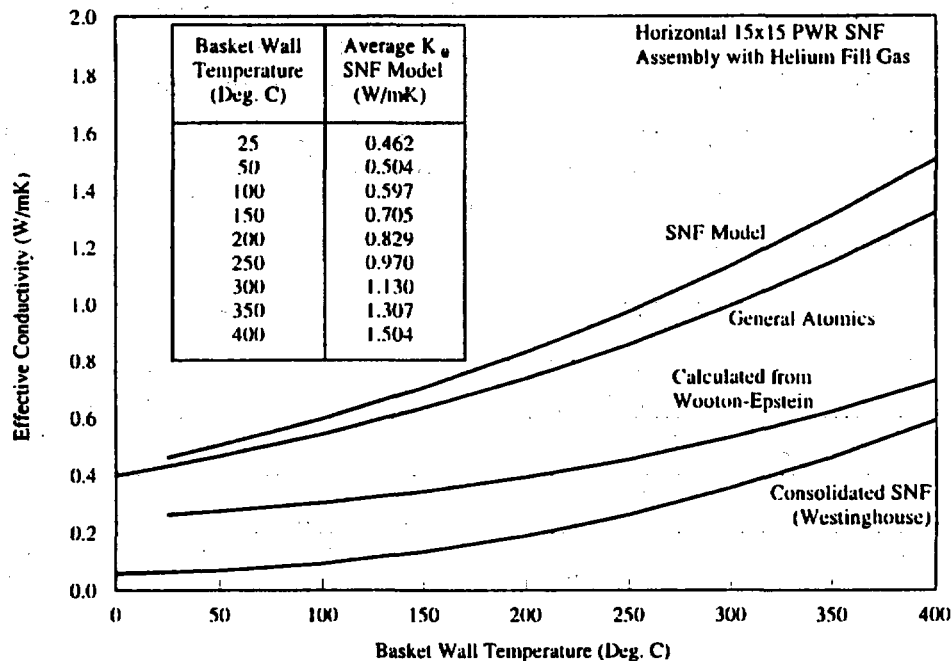


Figure 6.2-32. Spent Nuclear Fuel Effective Conductivities

6.2.1.2.5 SNF Model Benchmark Evaluations

Several benchmarking evaluations have been performed against performance tests conducted at the Idaho National Engineering Laboratory of the TN-24P (PNL 1987c), the Castor-V/21 (PNL 1986b), and the MC-10 (PNL 1987b) storage casks. Intact Westinghouse 15x15 PWR SNF assemblies were loaded into each of these casks at Idaho National Engineering Laboratory. Temperatures were measured with an array of thermocouples and compared to pre-test and post-test predictions with the COBRA-SFS and HYDRA-II heat transfer computer codes.

Presented here are the results of a benchmark of the SNF model against the performance test of the TN-24P (PNL 1987c) with helium fill gas in a horizontal configuration. To perform this benchmark, the SNF model was modified to represent the Westinghouse 15x15 PWR assembly (DOE 1992b). Besides slightly different assembly dimensions, the Westinghouse assembly also has 20 guide tubes, compared to 16 for the B&W assembly, which are in different positions.

The basket temperature and assembly heat load of assembly position D1 of the TN-24P test were chosen because D1 has the highest heat load of the four center assemblies. At the time the horizontal helium cask test was performed, this assembly (V18) generated about 911.2 W. To represent the basket temperature, thermocouple TC107 at the center of the basket was used. Its reported temperature for the horizontal helium run was 192.5°C, which was applied to the SNF model as the basket wall boundary condition.

Figure 6.2-33 displays the temperature contour results of this benchmark case with basket temperature from TC107 and heat load from assembly V18. To complete the benchmark, calculated guide tube temperatures are compared to those measured in the TN-24P test. The guide tube

thermocouple in assembly position D1-5 was TC9. Its reported temperature for the horizontal helium run was 206.2°C. Measured and calculated guide tube temperatures are compared in Table 6.2-12. Estimated peak cladding temperatures are also compared in Table 6.2-12. Peak cladding temperatures predicted by the SNF model are compared to peak cladding predictions performed by Pacific Northwest Laboratory using the COBRA-SFS code as part of the TN-24P testing (PNL 1987c). An additional calculation of estimated peak cladding temperature was also performed using the Wooton-Epstein correlation (Wooton-Epstein 1963).

Table 6.2-12. TN-24P Benchmark Test

	Calculated by SNF Model	Measured/Calc. in TN-24P Test	Calculated by Wooton-Epstein
Guide Tube	214.6°C	206.2°C	
Peak Cladding	221.1°C	215.0°C	247.7°C

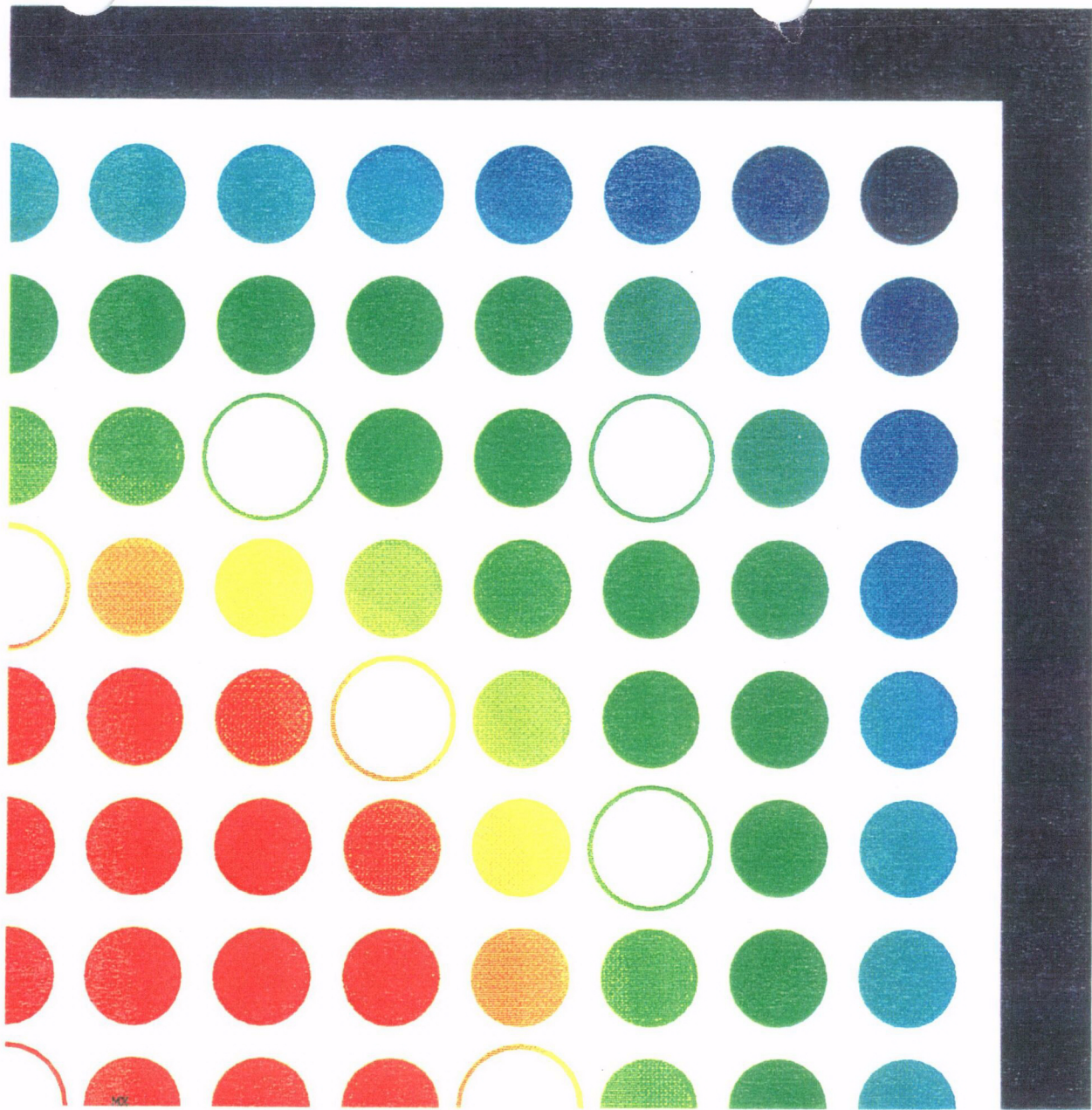
Table 6.2-12 demonstrates, again, the best estimate prediction with the SNF assembly model compared to conservative temperature predictions with the Wooton-Epstein correlation. Where the COBRA-SFS post-test slightly under-predicted guide tube temperatures in Figure 5-25 of the TN-24P report (PNL 1987c), the SNF model slightly over-predicted guide tube temperatures. While no thermocouple data are available for peak cladding temperatures for this test, the SNF model predicted cladding temperatures within 7°C of those predicted by the COBRA-SFS analysis. This benchmark test indicates that the SNF assembly model can accurately predict temperatures within a PWR assembly with a helium fill gas, and, therefore, can be used to derive effective conductivities for use in thermal analyses of WP designs in repository emplacement.

6.2.2 Criticality Analysis Basis

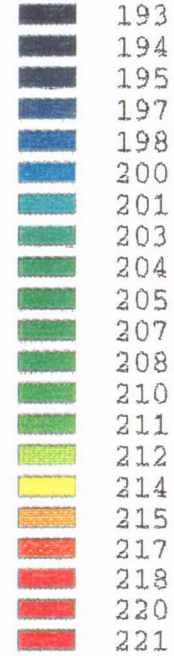
The following sections provide the basis for criticality analysis of the WP. The methods of criticality control are defined and the basic assumptions used to define the scope for criticality analyses are provided. The WP criticality analysis presented in Sections 6.3, 6.4, and 6.5 is based on the guidelines specified in this section.

6.2.2.1 Techniques Acceptable for Disposal Criticality Control

The nature of the MGDS project is such that many of the evaluations, analyses, and calculations being performed are first of a kind. When making evaluations of the technical feasibility of these criticality control techniques and strategies, a combination of preliminary calculations and engineering estimates is used when there are no hard scientific measurements or directly applicable engineering experience. Material testing and operational feasibility testing programs are underway and/or planned to generate the needed information. These tests will enable more informed estimates and give some definite answers to the technical viability of the strategies evaluated in this report. These evaluations and recommendations are based on the best engineering and scientific estimates currently available. The eight techniques evaluated are described below.



Temperature
Min ≈192.5
Max ≈221



Degrees C

911.2 Watts/assembly
195.5°C Basket Wall

Figure 6.2-33. TN-24P Benchmark Test Temperature Profile

C 20

1. **Burnup Credit** - The approach to criticality control that is considered most cost-effective because it requires no physical modification to the waste package. Also, it is less subject to concerns related to long-term material degradation. The approach takes credit for the net depletion of fissile material and the creation of neutron absorbing isotopes during the fission reaction. The criticality potential of SNF has been found to vary with cooling time. Deterministic models have been used to calculate the criticality potential of SNF out to a million years. These calculations show that the lowered reactivity (criticality potential) due to burnup is a valuable tool for long-term criticality control. Without burnup credit, the large capacity WPs are unlikely to be feasible for long-term disposal purposes. For large capacity WPs, burnup credit is normally considered in conjunction with other criticality control methods such as neutron absorber materials.
2. **Neutron Absorber Credit** - The use of supplemental neutron absorbing materials is also considered likely to be an acceptable approach for long-term criticality control. Neutron absorber materials placed in control panels and control rods (for PWR SNF assemblies) can provide a significant amount of negative reactivity (lower the system's criticality potential). However, for material performance reasons, credit for all the neutron absorber material loaded into a control system (panel or rod) is unlikely to be allowed. Neutron absorber credit is normally used as a primary criticality control measure only in reactors or SNF pools. For cask systems, neutron absorber credit is normally used in conjunction with other criticality control approaches. The MPC conceptual designs incorporate neutron absorber materials in both the burnup credit and flux trap designs.
3. **Moderator Displacement** - Considered likely to be a technically acceptable option for disposal criticality control. There are two concerns about the technical viability of using a filler material to displace moderator. The first concern is the amount of filler material required to displace enough water to control criticality. The amount is of concern due to limitations on how much filler can physically be inserted into the WP. The second concern is whether the filler material's performance characteristics will allow it to last over the time period of criticality control during isolation. Test programs are currently planned and/or underway to address these issues.

Moderator displacing filler material could be used alone or in conjunction with other criticality control approaches. It could be used as a replacement control measure where another measure is found inadequate for disposal.

4. **Reduced Capacity** - Controlling criticality by limiting the LWR SNF assembly capacity of a WP is also considered a technically acceptable approach for long-term criticality control. Without sufficient fissile material present in a package a criticality event cannot happen. The possibility of fissile material from multiple packages combining is considered unlikely (ORNL 1978). Reduced capacity could be used as the sole criticality control measure of a design. With this approach the WP is limited to a capacity of less than four PWR assemblies. Some of the SNF in the fuel inventory would further reduce the package capacities to one or two PWR assemblies, if additional control measures are

not used. Use of reduced capacity WPs on a large scale would be an economically unattractive alternative to use of filed large WPs.

5. **Basket Geometry, Separative Gaps (Flux Traps)** - Flux traps are *not* considered likely to be acceptable for disposal criticality control due to long-term material performance concerns. Testing is planned to prove or disprove the validity of these concerns. Flux trap designs depend on the structural materials to form the separative water gaps that control criticality. If the flux trap's separative gap collapses, the neutron interaction between fuel assemblies increases the criticality potential of the system. The structural performance of materials is one of the first physical properties lost as the materials degrade. After the containment barriers have failed, the basket structural materials lose their structural integrity over the period of isolation, and a flux trap will be unable to provide criticality control.

Flux trap designs are assumed filled with fresh fuel up to some initial enrichment limit. The initial enrichment limit is not sufficient control to prevent a package from going critical when a flux trap collapses, especially if it is to be able to accept 80 percent of the SNF inventory. The Flux Trap approach can be combined with other criticality control approaches to form hybrid strategies that may provide criticality control for disposal (i.e., provide sufficient neutron absorber to control criticality with collapsed flux traps).

6. **Moderator Exclusion** - *Not* considered acceptable for disposal criticality control. Moderator exclusion depends upon containment barriers to prevent water intrusion into the WP. The containment barriers cannot ensure the prevention of water inflow throughout the period of isolation.
7. **Rod Consolidation** - *Not* considered an acceptable option for disposal criticality control. There are concerns about the ability of the packaging to hold the fuel rods tightly together over the period of concern for criticality control. There are also concerns about the interactions between tightly packed fuel rods causing early failure and release of radionuclides (SNL 1987; SNL 1988; CRWMS M&O 1993f). Because of these and other concerns, rod consolidation has been dropped from consideration.
8. **Neutron Leakage/Reflection** - The use of neutron leakage/reflection as a major approach for long-term criticality control is *not* considered an acceptable option. Any neutron leakage that occurs is partially offset by the neutrons reflected back into a package from the surrounding water acting as a neutron reflector.

6.2.2.2 Approach For Evaluating Criticality Control

The Waste Package Development Department is developing an analysis methodology for evaluating disposal criticality. Once complete, the analysis methodology will be submitted to the Nuclear Regulatory Commission in a Topical Report for formal review and acceptance. The analysis methodology involves using two different calculational methods (deterministic and probabilistic) in a time-dependent, three-phased approach. A brief description of the two methods and how the methods fit in the three-phase approach is given below. The analysis methodology is still being

developed. The disposal criticality evaluations presented in this report are preliminary evaluations using only portions of the full analysis methodology.

6.2.2.2.1 Deterministic and Probabilistic Methodologies

Deterministic criticality evaluations are the type of evaluation currently performed for storage and transportation. The full deterministic criticality evaluation method involves calculating the criticality potential of a system using established design basis conditions/configurations. For deterministic evaluations, well defined conditions are imposed on a system, and the criticality potential of the system is calculated. The deterministic evaluation for transportation accidents, for example, fills the waste container with pure water (1g/cc) and places the fuel rods in their most reactive configurations.

Probabilistic criticality evaluations are a type of evaluation, similar to Probabilistic Risk Assessments performed for reactors. The full probabilistic criticality evaluation method involves using the probability of critical configurations occurring and the consequence of the particular criticality event occurring to determine an overall risk for criticality events. The probabilistic criticality methods currently envisioned would only determine the probability of sequences (or process chains) which lead to specific configurations that may credibly result in criticality. The probability distributions for the individual processes in a sequence would be based upon models of natural processes and/or material performance. The probabilities of final configurations are computed by combining the probabilities of the events and processes which lead to these configurations using standard techniques of risk analysis, including fault trees. The values of these probabilities will determine the credibility of the final configurations. The criticality potential of the credible configurations are determined using a deterministic criticality potential calculation.

The 10 CFR 60 criticality rule, as currently worded, does not clearly support a probabilistic method to demonstrate compliance. The Department of Energy has proposed to the Nuclear Regulatory Commission a change to the criticality rule that would invoke a probabilistically worded, performance-based postclosure criticality requirement. The proposed requirement would require that the probability and consequences of postulated criticalities provide reasonable assurance that repository performance objectives will be met. Discussions between the Department of Energy and Nuclear Regulatory Commission on this issue are ongoing.

6.2.2.2.2 Three-Phased Approach

As identified previously, 10 CFR 60.131(b)(7) addresses criticality control during the operation of the potential repository (preclosure) and the long-term criticality control requirements for isolation (postclosure). To better define the pre- and postclosure issues and the methodology for addressing them, a three-phased approach for disposal criticality control was developed. The three time phases associated with the approach are the Preclosure/Operations Phase, the Postclosure/Containment Phase, and the Postclosure/Isolation Phase.

- 1. Operations Phase -** Consists of approximately the first 100 years, which includes waste emplacement and the retrievability period. Human occupation is expected in the repository during this time frame. Therefore, during the preclosure/operations phase, criticality control is required to protect the health and safety of workers as well as that of the public.

Criticality control evaluations during this time phase are well suited to the use of a deterministic method. Deterministic criticality evaluations for the preclosure phase are similar to the evaluations performed for storage and transportation. Deterministic methods have been accepted by the Nuclear Regulatory Commission when evaluating system conditions that are well known and easy to define. Probabilistic methods may be used to determine the credible design basis configurations in the Engineered Barrier System.

2. **Containment Phase** - The time period from permanent closure to approximately 1,000 years postclosure. There is no human presence in the drifts and very few, if any, containment barriers have been breached. Therefore, the principal criticality concern is potential radionuclide release. The conditions at the start of the period are well defined; however, as time increases, the uncertainties in the condition of the WP and Engineered Barrier System increase. Probabilistic criticality evaluation methods (i.e., a probabilistic determination of potential critical configurations) will be used for this phase. The probabilistic method accounts for the uncertainty in conditions in the individual process probability distributions.
3. **Isolation Phase** - Anticipated to last from approximately 1,000 years postclosure to (currently) 10,000 years. The objective of criticality control during this time phase is to control radionuclide release into the environment. Probabilistic methods would be used for criticality evaluations during this time phase due to uncertainties associated with the integrity of the engineered barriers. A probabilistic risk-based criticality evaluation method to demonstrate compliance may become the logical choice for analyzing criticality during this phase, especially if the time period is extended beyond 10,000 years. The use of a risk-based demonstration method is dependant upon a change to the current, deterministically worded regulation.

6.2.2.3 Scope and Conditions of Criticality Control

The criticality control evaluations addressed in this report are concerned with long-term criticality control for the "conceptual design MPC", DHLW glass, and UCF WPs in a potential repository. The final disposal criticality analysis methodology has not been fully developed. The analysis method used to perform these evaluations is a preliminary methodology based upon parts of the complete disposal criticality analysis methodology. Deterministic evaluations of some potential configurations postulated by the preliminary probabilistic methods were performed. Criticality control evaluations for systems interior to the WP are the concern of this report. Criticality control evaluations for systems external to the WP will be addressed in other documents.

Trending deterministic evaluations were performed for the time periods covered by the three phases and beyond. Time effect evaluations concerned with changes to the composition and relatively minor geometric changes due to degraded materials are the only ones that have been analyzed to date. For this report, no criticality events involving degraded fuel assemblies or external accumulations to the WP have been evaluated. Both "normal" and "accident/off-normal" conditions are considered in the evaluations.

The "normal" condition in the repository, both within and surrounding the WP, is a dry environment. When an insufficient amount of water is present, insufficient neutrons are thermalized (slowed down to thermal energy levels) to bring a system critical. The k_{eff} of a standard WP under "normal" dry conditions is between 0.2 and 0.4. This k_{eff} is from the subcritical neutron multiplication caused by the subcritical neutron flux. Values of k_{eff} in this range do not represent a criticality safety concern, but are needed for shielding calculations.

The "accident/off-normal" condition considers the repository and WP as being flooded with water. Under flooded conditions, further detailed criticality evaluations of the system must be performed to determine k_{eff} . A WP fully flooded with cool (high-density) water is the standard WP criticality evaluation condition. This is the condition for which WP criticality evaluations are normally made, and is the condition assumed for most of the evaluations in this report. A preliminary parametric study of the reactivity effects of water density in the UCF WP has been performed in support of future probabilistic evaluations. This parametric analysis indicated that full-density water results in the highest k_{eff} value with and without boron in the basket structure (CRWMS M&O 1995aw).

The results of the analyses are dependent on the characteristics of the waste form in the WP. The reference PWR fuel assembly selected for CF and UCF development is the B&W 15x15 fuel type, which has been established as one of the more reactive PWR fuel designs under intact fuel assembly geometry conditions (CRWMS M&O 1994k). Various PWR and BWR assembly designs will be used in future calculations to demonstrate the most reactive type for specific waste package designs. The reference BWR fuel assembly is the GE 8x8 fuel type, which has been established as one of the more reactive BWR fuel designs under intact fuel assembly geometry conditions (CRWMS M&O 1994k). The reference DHLW glass form is the Savannah River Site HLW glass and pour canister, which is assumed representative of that from all DOE sites.

A number of important issues must be addressed for any WP design:

- The strategy of using "principal isotope" burnup credit supplemented by neutron absorber credit for criticality control must receive approval by the U. S. Nuclear Regulatory Commission to make the current designs viable.
- The criticality potential of SNF changes with time. The criticality potential initially decreases for the first 100 to 200 years, then increases to a local peak in the out years (approximately 10,000 to 20,000 years).
- Credible degradation of the basket/absorber material geometry must be considered and appropriate extra absorber material must be incorporated into the design to account for corrosion, leaching, and burnup. Current analyses for degraded scenarios are based on engineering judgement. Future calculations will be based on a full probabilistic analysis incorporating results from a number of engineering disciplines.
- The design analyses performed are based on design basis SNF, which currently covers approximately 97 percent of the SNF inventory. The level of inventory coverage significantly affects the engineered criticality control measures required in the design.

- The use of disposal control rod assemblies is a viable disposal criticality control measure for the majority of PWR SNF assemblies. Material performance tests will have to confirm their long-term acceptability.
- The results from the moderator displacement evaluations showed that the iron shot candidate filler material provides sufficient criticality control alone, but the viability of placing/dispersing a significant density of shot in a WP remains to be demonstrated.

6.2.3 Shielding Analysis Basis

The radiation shielding analyses are concerned with emplacement and disposal in the MGDS. Parametric and detailed analyses have been performed to analyze the different WP designs. The goal of parametric WP radiation shielding evaluations is to calculate the shielding requirements and/or dose rates for various shield materials, material thicknesses, and source terms for the WP designs. The shielding requirements and/or dose rates calculated in the parametric shielding evaluations are used to determine the effects of changing various components of the WP designs. Detailed analyses are performed on a preferred configuration based on the results of the parametric analyses.

The focus of the analyses provided in Sections 6.3, 6.4, and 6.5 is to provide dose rates from the WP as currently designed and to provide shielding thicknesses required for the transporter to allow for emplacement and handling. The emplacement transporter uses the incidental shielding of the WP and a shield carried on the WP emplacement transporter to reduce the dose rate. The transport shield can have optimized shield materials, which are not allowed around, or in, the emplaced WP. This strategy relies on remote handling operations.

The general design criteria to satisfy radiological protection and shielding requirements for the Geologic Repository Operations Area are specified in 10 CFR 60.131(a). This regulation indicates the design shall include suitable shielding. The acceptable dose rate criteria, specified in 10 CFR 20 (additional limits specified in the DOE *Radiological Control Manual*) (DOE 1994b), determine the amount of shielding needed for a given area. The performance objectives for radiological protection and shielding for the Geologic Repository Operations Area through permanent closure are specified in 10 CFR 60.111.(a). This regulation also mandates suitable shielding. The suitability of the shielding depends on the human occupation and equipment present, and the operations to be performed in the area being shielded. These details have not been established.

Material constraints make the shielding design effort more difficult. The MGDS requirements from 10 CFR 60.135 state the basic design criteria for the MGDS WP and its components. Neutron shielding materials in common use fail to meet two of the requirements of 10 CFR 60.135. The chemical composition (hydrocarbons, water, hydrogen) of the common shielding materials can accelerate the corrosion of the WP by microbiologically influenced corrosion and acidic dissolution of metals. In addition, the hydrocarbons are typically flammable. Furthermore, to conform with the Nevada state government's opposition to burying hazardous materials (e.g., lead) in an MGDS, the use of non-hazardous materials has been sought for the MGDS WP.

6.2.3.1 MGDS Target Dose Rates

Radiation shielding entails protecting workers and equipment from radiation sources. At this point in ACD activities, the radiation shielding for people is a concern. The work performed for these evaluations was aimed at computing and limiting dose rates to people. To comply with this goal, a target dose rate was established for WP radiation shielding.

Using a base of 250 work days per year or 2,000 hours per year and specifying up to one hour per day in the radiation field, the 10 CFR 20.1201(a)(i) 5 rem annual occupational dose limit allows a 20 mrem/hr radiation field. The initial target dose rate for MGDS activities was established at 20 mrem/hr at 2 m from the shield surface. The base 250 work days per year does not account for vacation or training time so some additional margin of safety exists for the target dose rate.

The established target dose rate incorporates some remote operations in the MGDS. For areas or positions that will require more time in the restricted radiation area, lower target dose rates will need to be established. For this reason the target dose rate listed above was lowered to 10 mrem/hr at 2 m for more recent calculations (two-dimensional). This dose rate is the same as that specified by the transportation regulation from 10 CFR 71 and would provide a lower bounds for applicaiton to repository operations. This dose rate would allow more direct access to WPs as far as radiation protection is concerned and is consistent with as-low-as-reasonably-achievable goals. Since these times and occupation positions are still being defined, the ACD activities have focused on using the 10 mrem/hr target dose rate.

The target dose rate for the fully self-shielding, shielding sleeve concept (discussed in the following section) has been lowered to 10 mrem/hr at 2 m. This dose rate is the same as that specified by the transportation regulation from 10 CFR 71. This dose rate would allow more direct access to WPs as far as radiation protection is concerned, but high temperatures near WPs may still limit any close proximity to the emplaced WPs.

Many of the current repository design concepts use shield doors between the access drifts (tunnels for human access) and emplacement drifts (the tunnels where WPs are emplaced). A preliminary dose rate of 0.25 mrem/hr on the access drift side of the shield doors for closed and filled emplacement drifts has been mentioned/discussed. The 0.25 mrem/hr dose rate corresponds to a 500 mrem annual exposure assuming 2,000 work hours per year. The 500 mrem annual exposure is a suggested general radiological criterion for new facilities from DOE *Radiological Control Manual* (DOE 1994b).

6.2.3.2 Strategies for Limiting Dose Rate

A basic property of the SNF and DHLW to be disposed in the MGDS is the high radioactivity. Because limiting the dose to workers is a major radiation protection goal (as low as reasonably achievable), methods for limiting the dose rate to workers have been devised. The two methods are shielding and remote handling. With these two methods, three strategies for limiting the dose rate from WPs are being considered: shielding WP sleeve, self-shielding containment barrier, and emplacement transport shield.

The shielding sleeve strategy places shield materials, specific to the shielding needs of the source, around the outer containment barriers of the disposal container in a "sleeve." In the case of SNF WPs, a concrete shielding sleeve has been considered. The shielding sleeve strategy would not necessarily need remote handling and would allow manned inspection of the WPs.

The self-shielding containment barrier strategy thickens the outer containment barrier to reduce the dose rate. The metallic outer barriers for the SNF WPs are not optimum neutron shields so the barriers must be quite thick. This strategy would require remote handling unless the additional weight and cost of an extremely thick containment barrier are acceptable.

The emplacement transport shield strategy uses the incidental shielding of the WP and a shield carried on the WP emplacement transporter to reduce the dose rate. The transport shield can have optimized shield materials, which are not allowed around, or in, the emplaced WP. This strategy relies on remote handling operations.

The *Engineered Barrier Design Requirements Document* (YMP, 1994b) indicates that shielding allocations between the repository segment and the Engineered Barrier System have not been determined. Currently, the WP is not required to be self-shielded. Calculations are performed for different options to give an indication of the tradeoff effects. A shielded transporter is the current preferred option and calculations are focused on evaluation of this option.

6.2.3.3 Scope of Radiation Shielding Calculations

The radiation shielding calculations needed to completely investigate the strategies and conditions of interest would require a significant time period to perform. Rather than taking all the possible combinations of calculations, a smaller set of calculations was performed. The radiation shielding calculations performed for these evaluations focused on the more limiting cases.

DHLW containers are expected from four sites and the characteristics of DHLW from each site are different. The radiation shielding calculations performed for the DHLW container evaluations focused on the Savannah River Site DHLW. It was chosen for the analyses because there is more information on the DHLW from Savannah River Site than the other sites.

Radiation exposure/dose rate information for human tissue (rem, mrem/hr) and computer chips rad (silicon) is needed. The human dose rates information takes precedence and is the current focus of the shielding evaluations. The rad (silicon) information for remote handling equipment will, however, be developed in the future.

A number of important issues must be addressed for any WP design:

- The WPs require shielding for only a relatively short amount of their lifetime. Providing shielding on a reusable platform such as the emplacement transporter is therefore more efficient and economical than incorporating the required shielding into the WP.

- The required transport shield thickness and weight impose additional carrying requirements on the emplacement transporter. These requirements can affect the type of transporter used in the MGDS. The calculated transporter shield thicknesses also indicate the shield requirements for movable "shadow" shielding or borehole shield plugs.
- The shielding design basis fuel is based on 10 years of decay time. The shielding requirements could be significantly reduced if an "aging" requirement were implemented in acceptance of fuel in the repository of more than 20 years.

INTENTIONALLY LEFT BLANK

6.3 UNCANISTERED FUEL DISPOSAL CONTAINER

The UCF disposal container is designed to contain and store SNF and/or non-fuel-bearing hardware delivered from nuclear reactor sites to the repository. The UCF disposal container system is intended to handle intact or damaged SNF from both PWR and BWR reactor types shipped to the MGDS repository in transportation casks that are not MPC-type containers. In addition, the UCF disposal container system will handle SNF shipped in MPC-type containers that does not meet the disposal acceptance requirements as packaged in the MPC and requires repackaging.

Upon arrival at the repository, the SNF or non-fuel-bearing hardware will be removed from the transportation cask and placed within a UCF WP. If necessary, filler material would be added at this time (note that use of filler material is a design option, and is not included in the nominal design). The UCF WP will then be sealed. The UCF WP conceptual design lifting feature consists of a lifting skirt at both ends of the disposal container. Each skirt has three holes placed at equal intervals and is designed to be adequate to lift the complete UCF WP (including filler material).

Design of the UCF WP is performed by the M&O Waste Package Development Department; the current UCF WP conceptual design is presented in Appendix B. The UCF WP will have different basket designs to handle PWR SNF, BWR SNF, damaged SNF, and non-fuel-bearing hardware shipped to the MGDS repository. The UCF WP design presented in this report emphasizes the disposal of SNF waste forms. Further design of the basket is required to handle the non-fuel-bearing waste that may be received. However, SNF will form the largest portion of the waste to be disposed.

6.3.1 Non-Fuel-Bearing Hardware

The term "non-fuel-bearing hardware" or "non-fuel components" may be defined broadly to cover all non-fuel-bearing components that receive radiation during power generation. Simply stated, non-fuel-bearing hardware is certain metallic materials that become radioactive after exposure to the neutron flux within the core of a nuclear reactor. Generally included are

- Components used to initiate, control, and monitor the chain reaction in the reactor core, often called non-fuel assembly hardware: neutron sources, control elements, burnable absorbers, in-core instrumentation, etc.
- Non-fuel portion of a fuel assembly, often called disassembly hardware: guide tubes, water rods, grids, nozzles, etc.
- Miscellaneous hardware used in the reactor core that is not a part of fuel assemblies: dummy assemblies, coupon trees, etc.

However, a more limited definition of non-fuel components has been adopted as follows: non-fuel-bearing hardware include, but are not limited to, control spiders, burnable poison rod assemblies, control rod elements, thimble plugs, fission chambers, and primary and secondary neutron sources contained within the fuel assembly; or BWR channels that are an integral part of the fuel assembly and do not require special handling. However, other components that do not meet these guidelines

will probably also be accepted, such as BWR control rods, which are between rather than within the SNF assembly, disassembly hardware, and other miscellaneous hardware.

Some non-fuel components may be stored within the SNF assembly, e.g., PWR control rods. However, a significant number of items, such as BWR control blades, cannot reasonably be stored as an integral part of the SNF assembly. These components may be crushed, segmented, or processed in some fashion to make the items easier to package for shipment and/or storage. Many reactor sites consolidate non-fuel components into canisters to ease tracking, storage, and collection. A canister is typically made of stainless steel or an inert alloy and placed in the SNF storage pools at the reactor site. When the canister is full, it is typically sealed with a lid, which is welded into place. Some reactor sites also use garbage or debris baskets. Thus, the non-fuel components hardware may arrive at the repository in any number of forms, which will have to be handled and placed into a UCF WP for MGDS disposal. The non-fuel components issue is intended to be handled by the UCF disposal container system. The process with which to handle this hardware will need to be addressed during the preliminary design.

6.3.2 Fuel-Bearing Hardware

Fuel-bearing hardware may be generally defined as any manufactured component that contains uranium or other fissionable heavy metal that is placed in a nuclear reactor core to create heat through the fission of the heavy metal. The most common and the largest portion of the waste is SNF; however, damaged SNF, consolidated fuel rods, experimental hardware, and other forms of waste also exist and are also considered fuel-bearing hardware. The UCF disposal container system is intended to handle all forms of fuel-bearing hardware and meet all criticality requirements for the MGDS repository. The conceptual designs currently emphasize intact SNF for both PWR and BWR reactor types. These SNF designs are well known and are characterized in Section 5. However, as the WP designs progress, consideration as to how to handle the small volume of other fuel-bearing hardware must be incorporated. However, the current basket designs for the WPs have been designed to handle the vast majority of the fuel-bearing waste forms.

6.3.3 Thermal Analysis

To capture a majority of the SNF, the WP must be designed and evaluated to accommodate the bounding or limiting case of SNF that has a thermal output much higher than average. Thus, a design basis SNF can be determined, which can be considered the hottest SNF that could be loaded and emplaced in that WP. The detailed WP/Engineered Barrier Segment thermal evaluation would then represent the hottest WP in the repository at a given thermal loading with average SNF. While all of the WPs (hot and cold) will collectively influence repository temperatures (average SNF characteristics), every WP must meet thermal goals (design basis SNF characteristics). The methodology and selection of design basis SNF for WP design is covered in Section 5.

Given that higher-capacity WPs are more likely to exceed thermal goals than smaller ones in the same repository thermal environment, the choice of a design basis SNF is important because it could limit the number of assemblies that can be loaded without exceeding thermal goals for disposal. The limiting thermal goal for large WPs, such as the 21 PWR UCF WP, is a temperature of no more than 350°C at the SNF cladding. Design bases have been established for WP design based on the total

potential repository inventory (CRWMS M&O 1994j). The design basis SNF types that have been used in the following thermal analyses to demonstrate compliance with requirements and to allow comparison with previous evaluations are summarized in Table 6.3-1. Figure 6.2-4 in Section 6.2.1.1 compared the time-dependent heat decay for each of the SNF types.

Table 6.3-1. Uncanistered Fuel Waste Package Thermal Analysis Design Basis

Organization	SNF Type	SNF Age	SNF Burnup	Initial Heat
MGDS	PWR	10 years	48 GWd/MTU	850 W
MGDS	BWR	10 years	49 Gwd/MTU	409 W

Design basis SNF will impact the timing of peak temperatures, as well as the magnitude of the peak. The repository host rock temperatures will peak between 10 and 500 years, depending on the thermal loading, but will be largely independent of the individual WP design. The WP itself will experience its peak temperature before the rock temperature peaks. The peak temperature and its timing will depend on the design basis SNF and the basket/container design. In previous analyses of the large WP (CRWMS M&O 1994i), higher conductivity SNF baskets were seen to lower and delay the peak temperatures experienced. The choice of the design basis SNF is of key importance. Younger SNF types produce high peak temperatures within the first year, then drop off quickly. Older SNF (at the same initial areal power density, but not areal mass loading) produces lower and later peaks with more stable and higher long-term temperatures. In the following evaluations, more than one design basis SNF type has been used to illustrate the impacts of the SNF types.

A second key factor in evaluating internal WP temperatures is the determination of peak cladding temperatures. Three methods are available to estimate cladding temperatures inside a storage, transportation, or disposal container. The first and most involved method is to explicitly model the canister and every fuel rod in every assembly within it. This model would directly consider the internal fill gas convection and conduction, and a matrix of radiation view factors among the rods. The second method employs the Wooton-Epstein correlation (Wooton-Epstein 1963) to estimate the peak cladding temperature based on the highest steady state temperature in the SNF basket structure. The Wooton-Epstein correlation has historically been the primary tool of transportation/storage cask vendors as it simplifies the analysis and has been previously accepted by the U.S. Nuclear Regulatory Commission. The third method of estimating peak cladding temperatures is to prepare a finite-element or finite difference model of the SNF assembly volume as a smeared solid with internal volumetric heat generation as part of the entire disposal container model. An effective conductivity for the assembly volume can be defined that will approximate the temperature drop across a PWR assembly.

The key to accurate SNF cladding temperature predictions using the effective conductivity method lies in determining the proper conductivity to assume in the assembly volume. Section 6.2.1.2 describes the development of an ANSYS SNF assembly model for the determination of effective conductivities. The temperature-dependent conductivities reported in that section were applied to the homogeneous assembly volumes in the following UCF WP thermal evaluations. The peak assembly temperatures using the effective conductivity provide a "best estimate" for peak clad

temperatures, which is compared for each case to "conservative" estimates of cladding temperatures using the Wooton-Epstein correlation.

The use of filler material could also affect the determination of WP internal temperatures. The thermal effects of adding filler material to the WP have previously been investigated (CRWMS M&O 1994i). While the addition of material to fill the void space within the WP may be beneficial to criticality control and containment (by inhibiting corrosion and radionuclide release), the thermal effects depend entirely on the type and conductivity of the material used. Iron shot was found not to have a significant effect on peak temperatures; however, other less conductive materials could seriously affect large UCF WP where internal temperatures can approach maximum thermal goals.

6.3.3.1 21 PWR UNCANISTERED FUEL WASTE PACKAGE

A two-dimensional finite-element thermal model of the large 21 PWR burnup credit UCF WP conceptual design was developed by the M&O Waste Package Design Group. Model detail including the separate layers of the basket tube design for each disposal container design is provided with the figures in Appendix B. Intimate contact was assumed between the layers of stainless steel and aluminum, and also between the tube guides and inner shell. The UCF WP fill gas was assumed to be helium. The analysis is described in detail in a supporting design analysis (CRWMS M&O 1995s).

The finite-element code ANSYS was used to model the two-dimensional cross-section of the UCF WP. Time and position-dependent temperatures for the WP surface were exported from the emplacement model, described in Section 6.2.1.1.1, and applied as time-varying boundary conditions. The other time-varying conditions used in the model were the design basis SNF decay heat outputs applied as volumetric heat generations to the assembly areas of the model and use smeared material properties. The effective conductivity for the assembly area was developed as described in Section 6.2.1.2; it represents the resistance due to heat transfer in a 15x15 PWR assembly. The heat loads for the assembly areas were interpolated from the Oak Ridge database of SNF characteristics for each of the assumed design basis SNF types. The heat load will decrease logarithmically with time as the fission products decay. The heat loads were applied volumetrically and were multiplied by an axial heat peaking factor to approximate the axial center of the WP with a two-dimensional model. An SNF assembly is much hotter at the mid-length than at the ends, and it is conservative to assume the two-dimensional WP model represents the hottest cross-section of the UCF WP.

The boundary conditions and heat loads were applied and solved out to 1,000 years for each of the five thermal loading scenarios described in Section 6.2.1.1.1 and for each of the PWR design basis SNF types described in Table 6.3-1. Table 6.3-2 summarizes the peak temperatures and the time of occurrence for each of the cases analyzed. The thermal loading scenarios indicated in Table 6.3-2 are defined in Table 6.2-1, and the design basis SNF descriptions are provided in Table 6.3-1. Both "conservative" estimates of peak cladding temperatures using the Wooton-Epstein correlation, and "best estimate" predictions using the effective conductivity method are presented in the table. Peak

Table 6.3-2. 21 PWR UCF WP Thermal Analysis Results

Thermal Load	Design Basis SNF	Peak Cladding				Peak Basket		WP Surface	
		Conservative Estimate		Best Estimate		°C	yrs	°C	yrs
		°C	yrs	°C	yrs				
High #1	MGDS	272	8	251	8	234	10	188	50
High #2	MGDS	263	5	241	8	223	8	165	40
Low #1	MGDS	250	0.9	224	1	201	2	117	8
Low #2	MGDS	256	2	231	2	210	3	131	8
Low #3	MGDS	265	3	241	3	221	5	146	10

cladding temperatures using effective conductivity are calculated directly in the ANSYS program, and Wooton-Epstein calculations for each time step in the ANSYS analysis were also performed for comparison.

The thermal history for the MGDS thermal design basis SNF at 83 MTU/acre is presented in Figure 6.3-1. Figure 6.3-2 displays the temperature profile across the UCF SNF basket and disposal container for the time of peak internal temperatures (eight years). The peak estimate for high thermal loading #2 SNF cladding temperature was 241 °C, which can be compared to the estimate of 263 °C, which was calculated with the Wooton-Epstein correlation.

In a previous M&O report (CRWMS M&O 1994i), the WP surface temperature was predicted to be 205 °C, which resulted in higher cladding temperature predictions for that analysis. That analysis was also specific to the MPC conceptual design. There are two reasons for environment temperatures lower than 205 °C in the current evaluation. First, and primarily, the WP spacing has been increased from 16 m to 19.5 m to accommodate a 22.5 m drift spacing. A greater WP spacing results in lower near-field temperatures, as described in Section 6.2.1.1.1. Second, the previous analysis used a two-dimensional repository emplacement thermal model, which, compared to a three-dimensional model, over-predicted near-field temperatures. In general, as more information becomes available and modeling techniques are improved, conservatism will be replaced with greater accuracy in the evaluations.

Peak temperatures inside the WP occur between the time of emplacement and the time of peak drift wall temperatures. At emplacement, the SNF heat load is at its highest, but the drift is still cool, and by the time of peak drift temperatures, the heat load has decayed so that internal temperature drops are lower. As indicated in Table 6.3-2, the time of peak temperatures varies depending on thermal loading, WP spacing, SNF basket design, and the time-dependent WP decay heat (SNF type). For most design basis SNF types, peak WP internal temperatures will occur in less than five years after emplacement even though WP surface temperatures do not peak for 40 years or more.

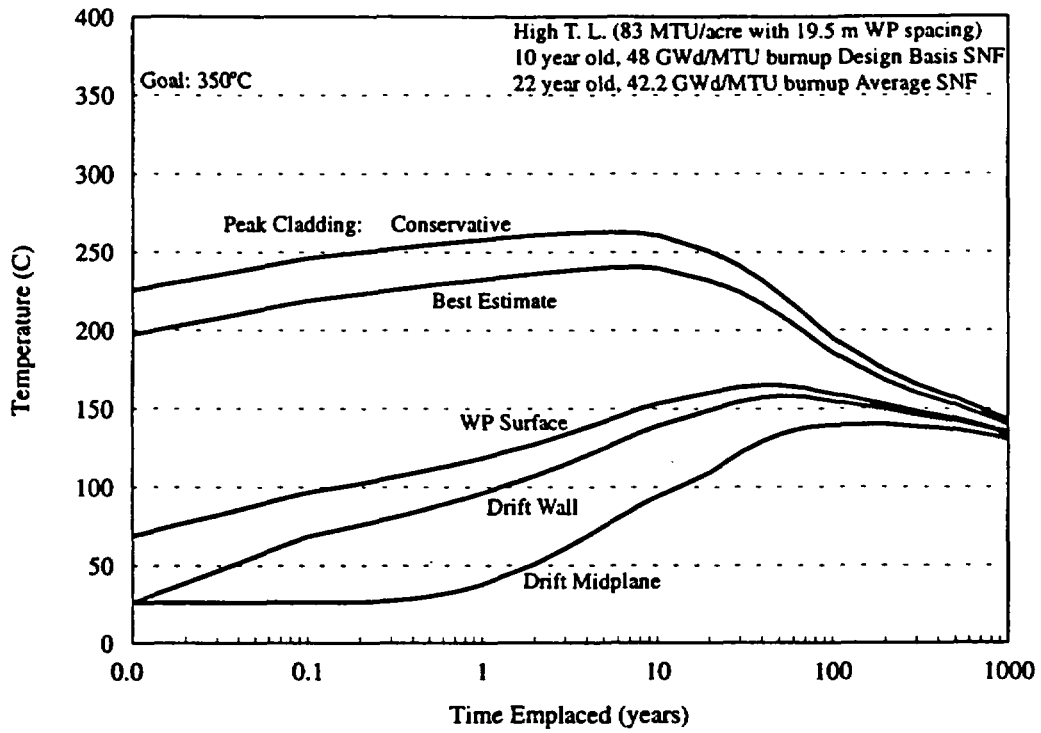


Figure 6.3-1. 21 PWR UCF, High Thermal Loading (#2), MGDS Design Basis Fuel

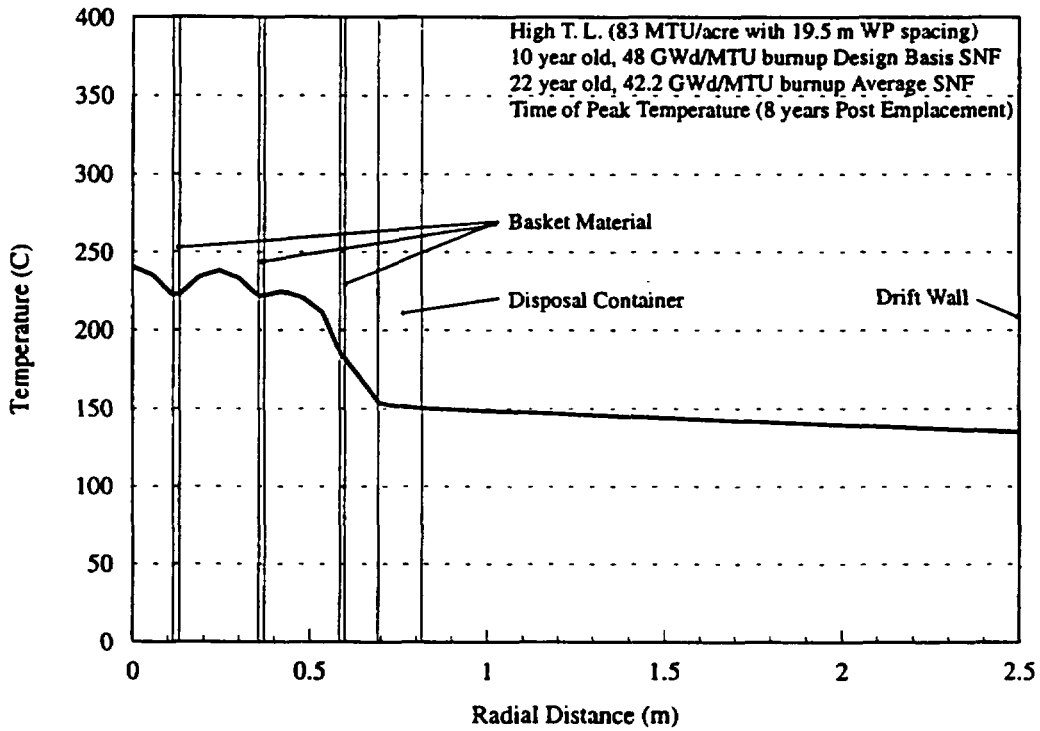


Figure 6.3-2. Temperature Profile in 21 PWR UCF

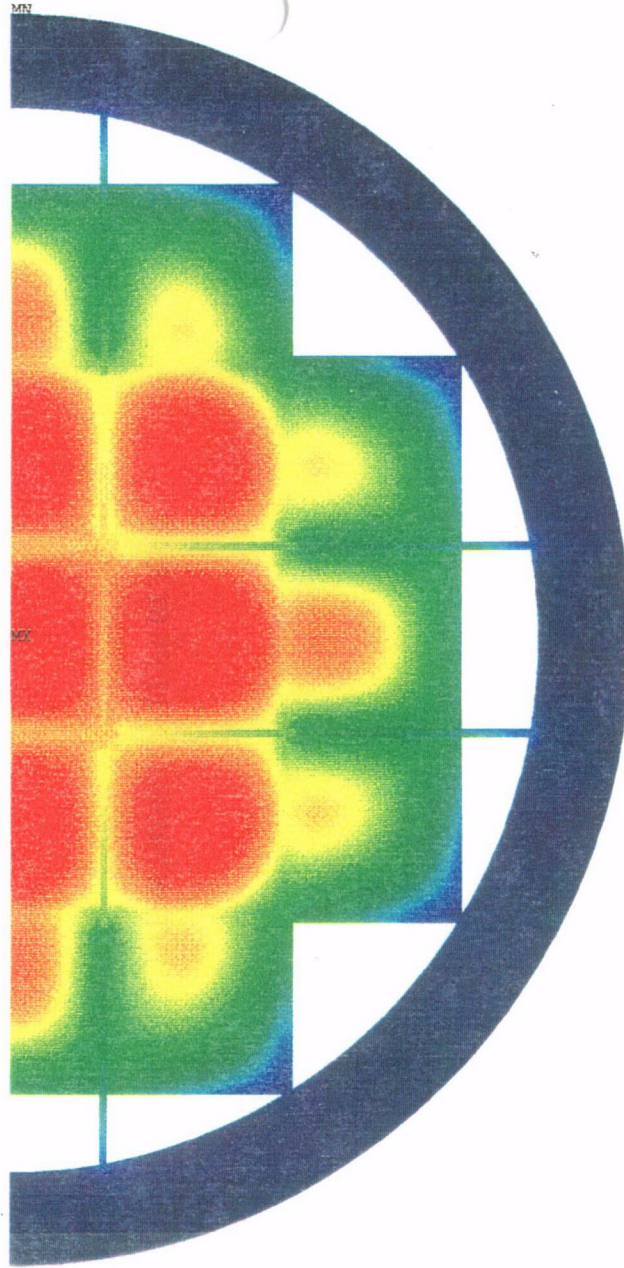
Figure 6.3-3 displays the temperature contours in the 21 PWR UCF WP at the time of peak temperatures, eight years. The thermal loading for this case was 83 MTU/acre (20.5 kgU/m²) and the MGDS design basis SNF was assumed. Figures 6.3-4, 6.3-5, and 6.3-6 display the temperature contours for the same case at 10, 50, and 100 years, respectively. By 100 years, the temperature drop across the WP (from center to edge) has dropped to less than 30°C.

While 83 MTU/acre is considered a more likely scenario for a high thermal loading, a higher thermal loading of 100 MTU/acre was also evaluated to bound the WP internal temperatures for the full range of possible thermal loadings. Figure 6.3-7 displays the thermal history of the 21 PWR UCF WP at 100 MTU/acre (24.7 kgU/m²) for the MGDS thermal design basis SNF. This combination of a short WP spacing and a high thermal loading resulted in the highest temperatures of all of the cases considered. SNF cladding temperatures peaked at 251°C (272°C using Wootton-Epstein) and average repository horizon temperatures remained above 150°C past 1,000 years. Calculations at Lawrence Livermore National Laboratory (LLNL 1994b) have shown that above-boiling conditions will persist for thousands of years at areal mass loadings in this range; however, some temperatures are close to limiting thermal goals.

Figure 6.3-8 displays the thermal history of the 21 PWR UCF WP at a low thermal loading of 25 MTU/acre (6.2 kgU/m²) with the long WP spacing (low thermal load #1) for the MGDS thermal design basis SNF. Peak internal temperatures are similar to those for the high thermal loading because the peaks occur in the first few years before any effects of thermal loading have been realized. Figure 6.3-9 displays the thermal history of the 21 PWR UCF WP for low thermal load #2 for the MGDS thermal design basis SNF. Because the WP spacing is similar to that for high thermal load #2, similar temperatures are predicted for the first few years of emplacement. However, as thermal loading effects emerge, all of the low thermal loading results converge as described in Section 6.2.1.1.1. Figure 6.3-10 displays the thermal history of the 21 PWR UCF WP for low thermal load #3 for the MGDS thermal design basis SNF. The highest internal temperature for all cases occurred where the MGDS thermal design basis SNF is modeled and the shortest WP spacing (16.2 m) defines the thermal loading. The peak temperatures occur before drift-to-drift effects emerge such that WP spacing drives the peak near-field temperatures and high thermal load #1 and low thermal load #3 have nearly the same peak cladding temperature.

The thermal evaluation of the 21 PWR UCF WP conceptual design with respect to the repository has considered a number of thermal loading scenarios. The repository thermal loading has not been specified and will not be finally established for years. Therefore, the WP thermal behavior has been analyzed for a range of thermal loadings. For each repository thermal loading scenario, a three-dimensional repository emplacement and two-dimensional WP evaluation were performed. Results of the thermal evaluations indicate that the 21 PWR UCF WP design satisfies the thermal limitations for disposal in the MGDS.

INTENTIONALLY LEFT BLANK



ANSYS 5.0 A
JUN 12 1995

Temperature

Min =149

Max =241

- 150
- 154
- 159
- 164
- 168
- 172
- 177
- 181
- 186
- 191
- 195
- 199
- 204
- 208
- 213
- 218
- 222
- 226
- 231
- 236
- 241

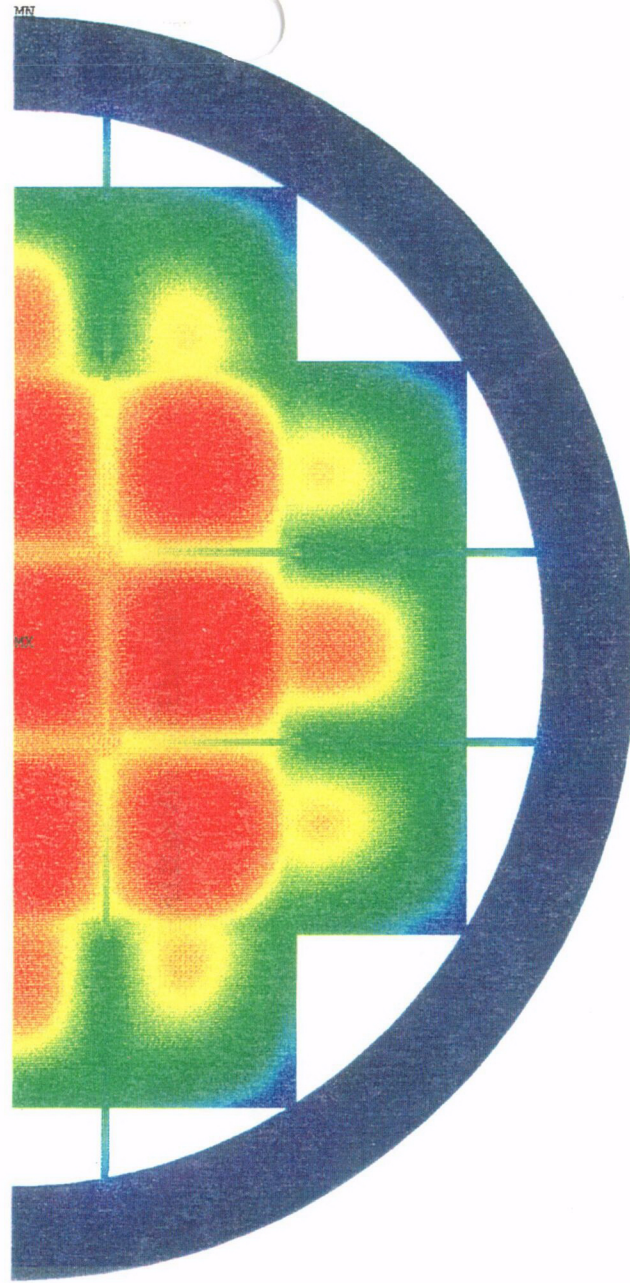
Degrees C

83 MTU/acre

10-year-old SNF
48 GWd/MTU

C21

Figure 6.3-3. 21 PWR UCF Peak Temperatures (8 Years)

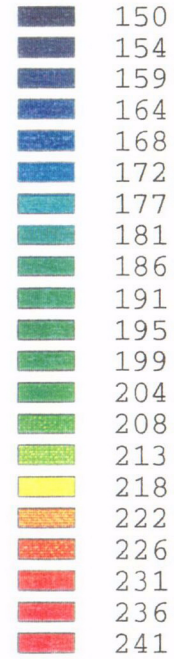


ANSYS 5.0 A
JUN 12 1995

Temperature

Min =152

Max =240



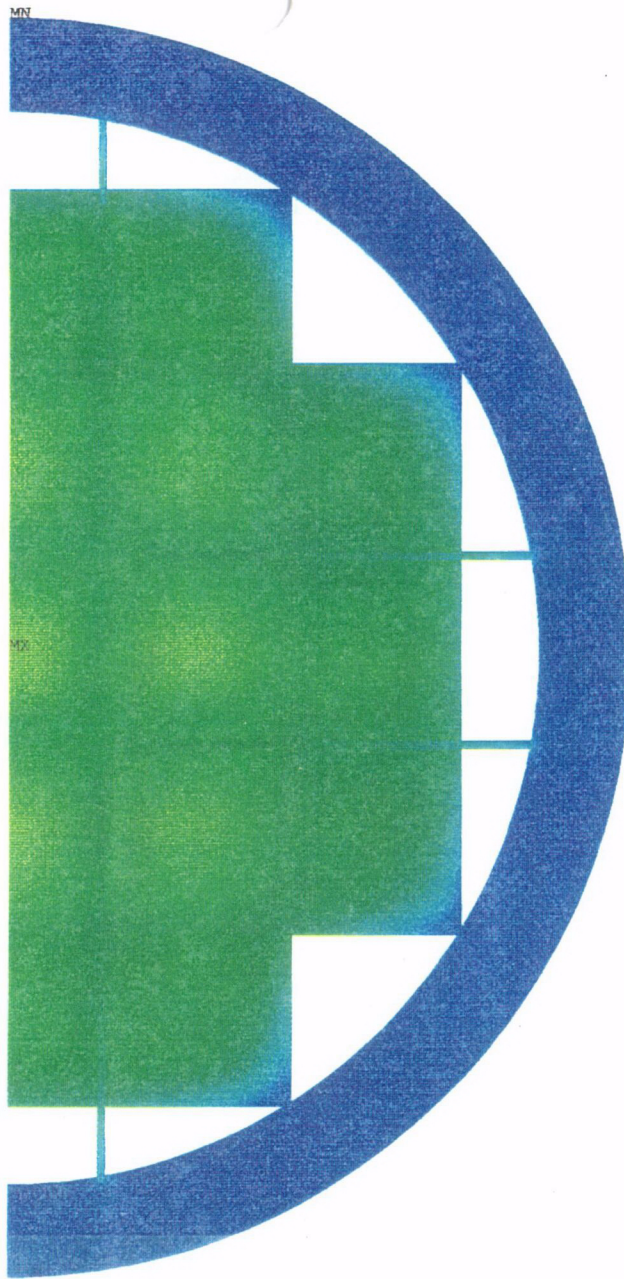
Degrees C

83 MTU/acre

10-year-old SNF

48 GWd/MTU

Figure 6.3-4. 21 PWR UCF Temperatures at 10 Years



ANSYS 5.0 A
JUN 12 1995

Temperature

Min =164

Max =210

- 150
- 154
- 159
- 164
- 168
- 172
- 177
- 181
- 186
- 191
- 195
- 199
- 204
- 208
- 213
- 218
- 222
- 226
- 231
- 236
- 241

Degrees C

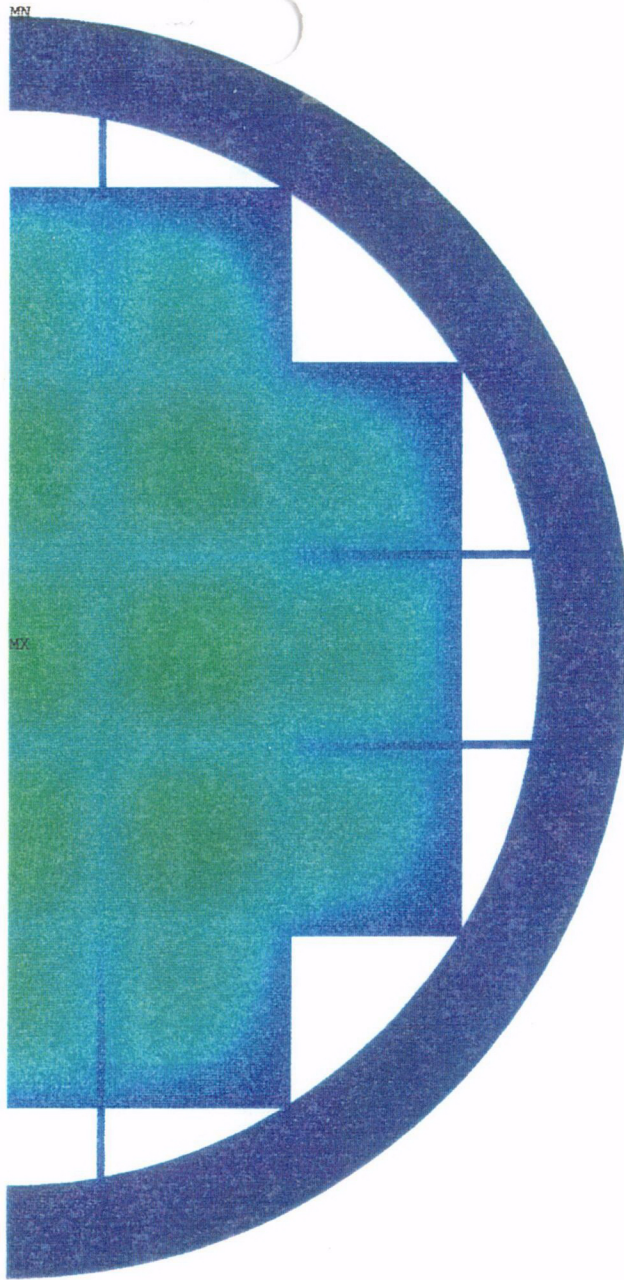
83 MTU/acre

10-year-old SNF

48 GWd/MTU

23

Figure 6.3-5. 21 PWR UCF Temperatures at 50 Years



ANSYS 5.0 A
JUN 12 1995

Temperature

Min =159

Max =185

- 150
- 154
- 159
- 164
- 168
- 172
- 177
- 181
- 186
- 191
- 195
- 199
- 204
- 208
- 213
- 218
- 222
- 226
- 231
- 236
- 241

Degrees C

83 MTU/acre

10-year-old SNF

48 GWd/MTU

24

Figure 6.3-6. 21 PWR UCF Temperature at 100 Years

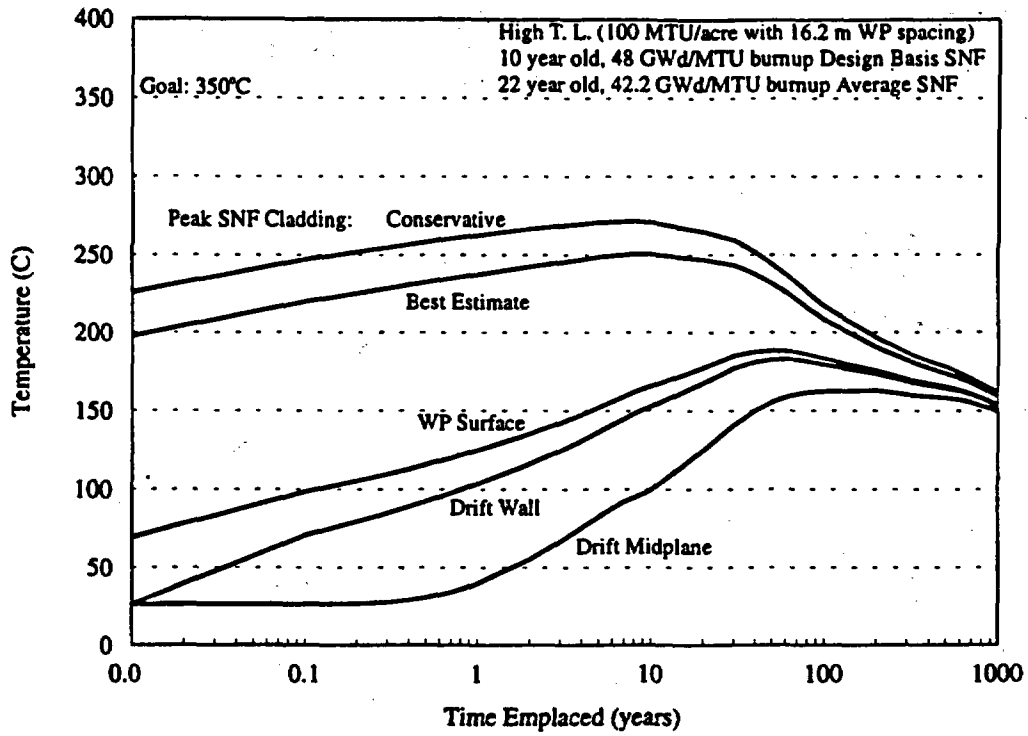


Figure 6.3-7. 21 PWR UCF, High Thermal Load (#1), MGDS DBF

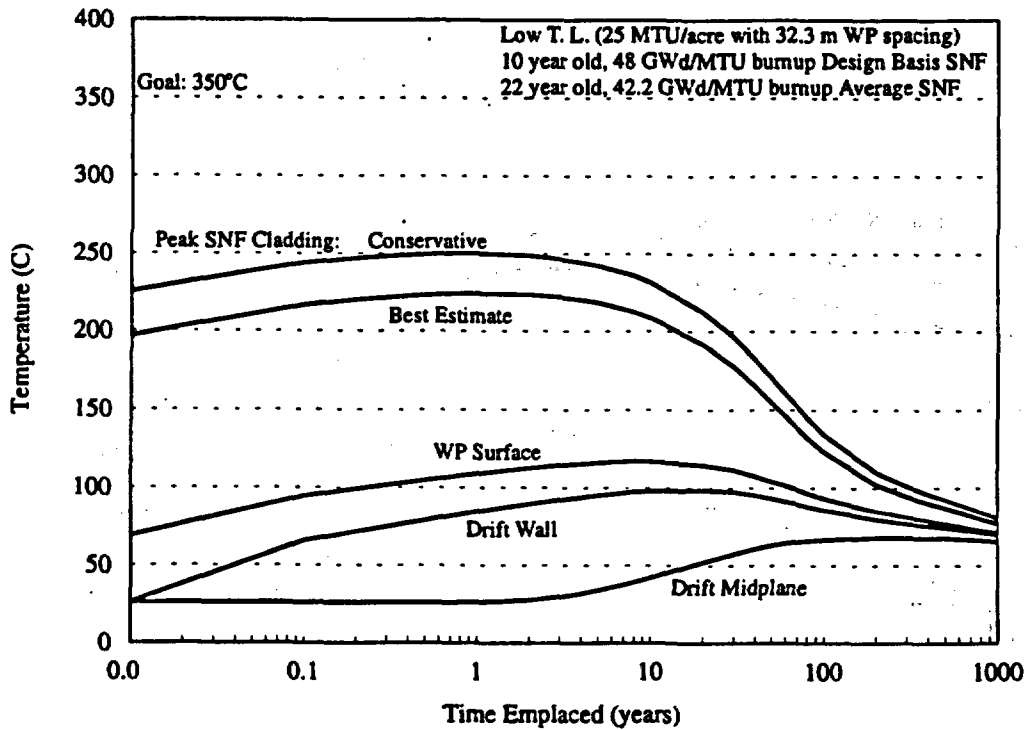


Figure 6.3-8. 21 PWR UCF, Low Thermal Load (#1), MGDS DBF

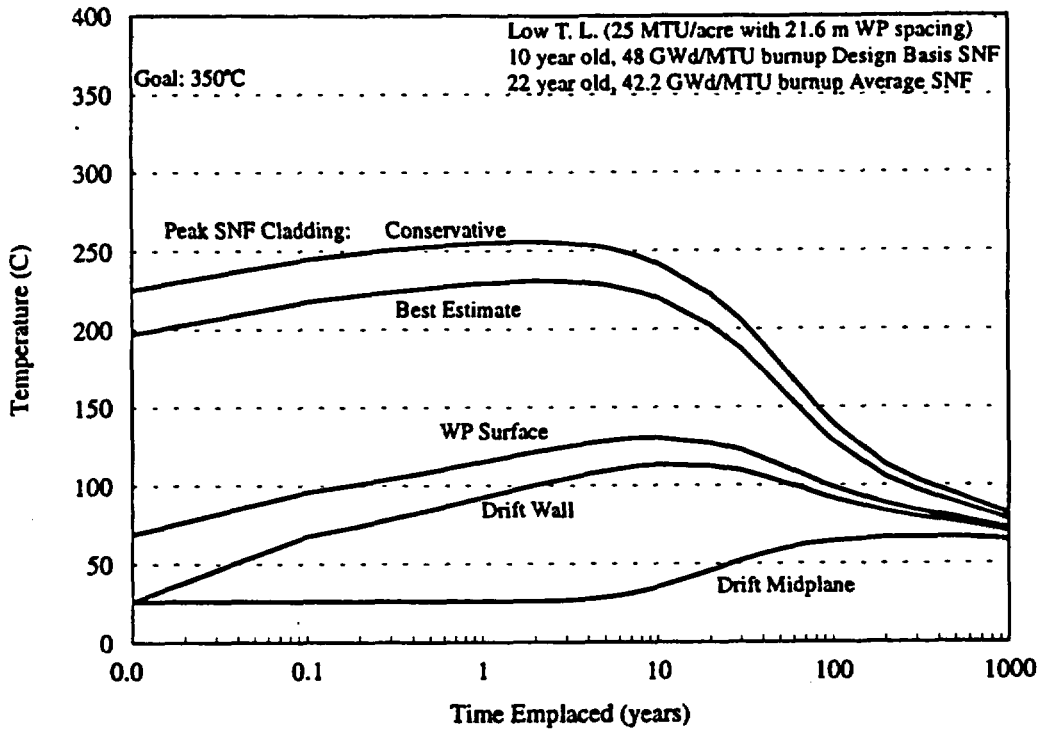


Figure 6.3-9. 21 PWR UCF, Low Thermal Load (#2), MGDS DBF

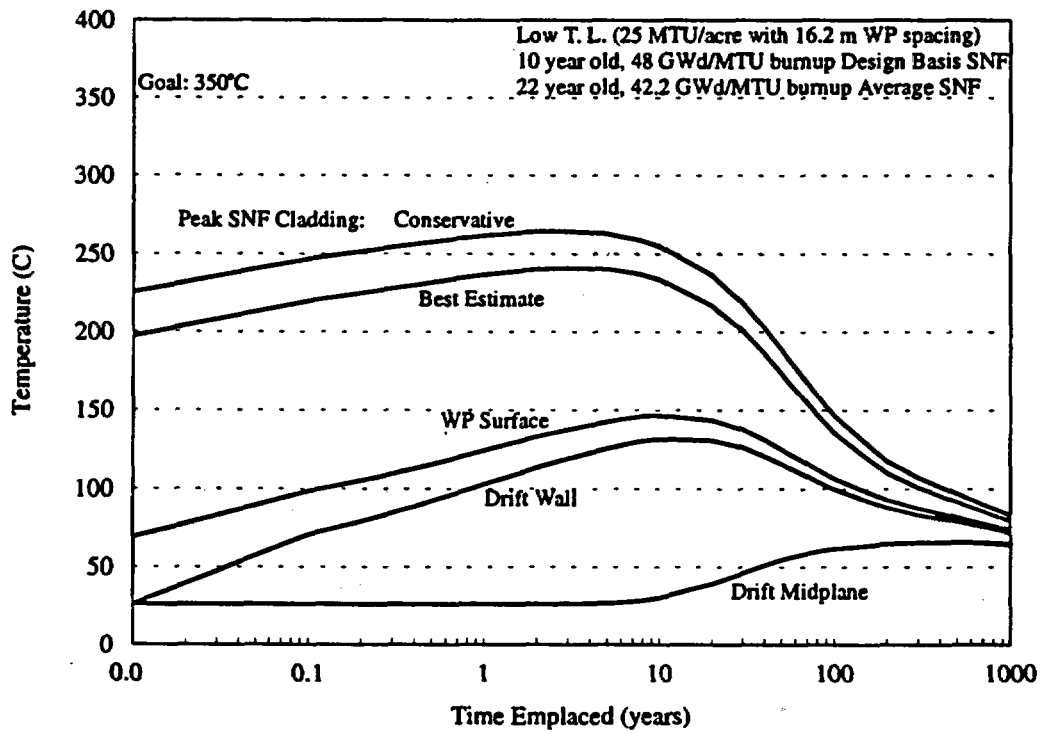


Figure 6.3-10. 21 PWR UCF, Low Thermal Load (#3), MGDS DBF

6.3.3.2 12 PWR UNCANISTERED FUEL WASTE PACKAGE

A two-dimensional finite-element thermal model of the small 12 PWR UCF WP conceptual design was developed by the M&O Waste Package Design Group. Model detail including the separate layers of the basket tube design for each disposal container design is provided with the figures in Appendix B. Intimate contact was assumed between the layers of stainless steel and aluminum, and also between the tube guides and inner shell. The UCF WP fill gas was assumed to be helium. The analysis is described in detail in a supporting design analysis (CRWMS M&O 1995t).

The finite-element code ANSYS was used to model the two-dimensional cross-section of the UCF WP. Time and position-dependent temperatures for the WP surface were exported from the emplacement model, described in Section 6.2.1.1.2, and applied as time-varying boundary conditions. The other time-varying conditions used in the model were the design basis SNF decay heat outputs applied as volumetric heat generations to the assembly areas of the model and use smeared material properties. The effective conductivity for the assembly area was developed as described in Section 6.2.1.2; it represents the resistance due to heat transfer in a 15x15 PWR assembly. The heat loads for the assembly areas were interpolated from the Oak Ridge database of SNF characteristics for each of the assumed design basis SNF types. The heat load will decrease logarithmically with time as the fission products decay. The heat loads were applied volumetrically and were multiplied by an axial heat peaking factor to approximate the axial center of the WP with a two-dimensional model. An SNF assembly is much hotter at the mid-length than at the ends, and it is conservative to assume the two-dimensional WP model represents the hottest cross-section of the UCF WP.

The boundary conditions and heat loads were applied and solved out to 1,000 years for each of the five thermal loading scenarios described in Section 6.2.1.1.2 and for each of the PWR design basis SNF types described in Table 6.3-1. Table 6.3-3 summarizes the peak temperatures and the time of occurrence for each of the cases analyzed. The thermal loading scenarios indicated in Table 6.3-3 are defined in Table 6.2-2, and the design basis SNF descriptions are provided in Table 6.3-1. Both "conservative" estimates of peak cladding temperatures using the Wooton-Epstein correlation, and "best estimate" predictions using the effective conductivity method are presented in the table. Peak cladding temperatures using effective conductivity are calculated directly in the ANSYS program, and Wooton-Epstein calculations for each time step in the ANSYS analysis were also performed for comparison.

The thermal history for the MGDS thermal SNF at 83 MTU/acre (20.5 kgU/m²) is presented in Figure 6.3-11. Figure 6.3-12 displays the temperature profile across the UCF basket and disposal container for the time of peak internal temperatures (10 years). The peak estimate for high thermal loading #2 SNF cladding temperature was 217°C, which can be compared to the estimate of 243°C that was calculated with the Wooton-Epstein correlation. Both SNF cladding temperature estimates are comfortably below the cladding temperature limit of 350°C.

Table 6.3-3. 12 PWR UCF WP Thermal Analysis Results

Thermal Load	Design Basis SNF	Peak Cladding				Peak Basket		WP Surface	
		Conservative Estimate		Best Estimate		°C	yrs	°C	yrs
		°C	yrs	°C	yrs				
High #1	MGDS	253	8	229	20	218	30	184	60
High #2	MGDS	243	8	217	10	202	10	160	50
Low #1	MGDS	223	1	191	2	171	2	101	20
Low #2	MGDS	233	2	202	3	184	4	118	10
Low #3	MGDS	244	3	215	5	198	5	137	10

Figure 6.3-13 displays the temperature contours in the 12 PWR UCF WP at the time of peak temperatures, 10 years. The thermal loading for this case was 83 MTU/acre (20.5 kgU/m²) and the MGDS thermal design basis SNF was assumed. Figures 6.3-14 and 6.3-15 display the temperature contours for the same case at 50 and 100 years, respectively. By 100 years, the temperature drop across the WP (from center to edge) has dropped to less than 25°C.

While 83 MTU/acre is considered a more likely scenario for a high thermal loading, a higher thermal loading of 100 MTU/acre was also evaluated to bound the WP internal temperatures. Figure 6.3-16 displays the thermal history of the 12 PWR UCF WP at 100 MTU/acre (24.7 kgU/m²) for the MGDS thermal design basis SNF. This combination of a short WP spacing and high thermal loading resulted in the highest temperatures of all of the cases considered. SNF cladding temperatures peaked at 229°C (253°C using Wooton-Epstein) and average repository horizon temperatures remained above 150°C for hundreds of years. Just as for the 21 PWR UCF WP cases, above-boiling, near-field temperatures persisted past 1,000 years.

Figure 6.3-17 displays the thermal history of the 12 PWR UCF WP at low thermal loading of 25 MTU/acre (6.2 kgU/m²) with the long WP spacing (low thermal load #1) for the MGDS thermal design basis SNF. As with the 21 PWR UCF WP, peak internal temperatures are similar to those for the high thermal loadings because the peaks occur before any effects of thermal loading have been realized. Figure 6.3-18 displays the thermal history of the 12 PWR UCF WP for low thermal load #2 for the MGDS thermal design basis SNF. Because the WP spacing is similar to that for high thermal load #2, similar temperatures are predicted for the first few years of emplacement. Figure 6.3-19 displays the thermal history of the 12 PWR UCF WP for low thermal load #3 for the MGDS thermal design basis SNF. The highest internal temperature occurred where the MGDS thermal design basis SNF is modeled and the shortest WP spacing (9.2 m) defines the thermal loading. The peak temperatures occur before drift-to-drift effects emerge such that the WP spacing drives the peak near-field temperatures and high thermal load #1 and low thermal load #3 have nearly the same peak cladding temperatures.

The thermal evaluation of the 12 PWR UCF WP conceptual design with respect to the repository has considered a number of thermal loading scenarios. The repository thermal loading has not been specified and will not be finally established for years. Therefore, the WP thermal behavior has been analyzed for a range of thermal loadings. For each repository thermal loading scenario, a three-dimensional repository emplacement and two-dimensional WP evaluation were performed. The results of the thermal evaluations indicate that the 12 PWR UCF WP design satisfies the thermal limitations for disposal in the MGDS.

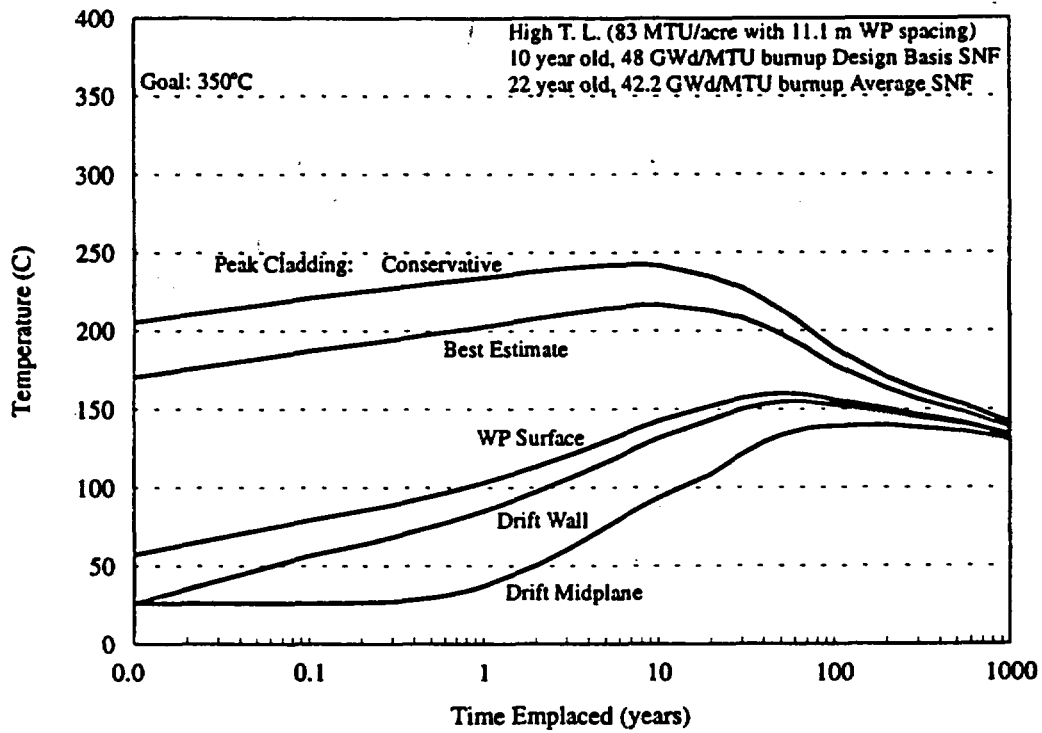


Figure 6.3-11. 12 PWR UCF, High Thermal Load (#2), MGDS DBF

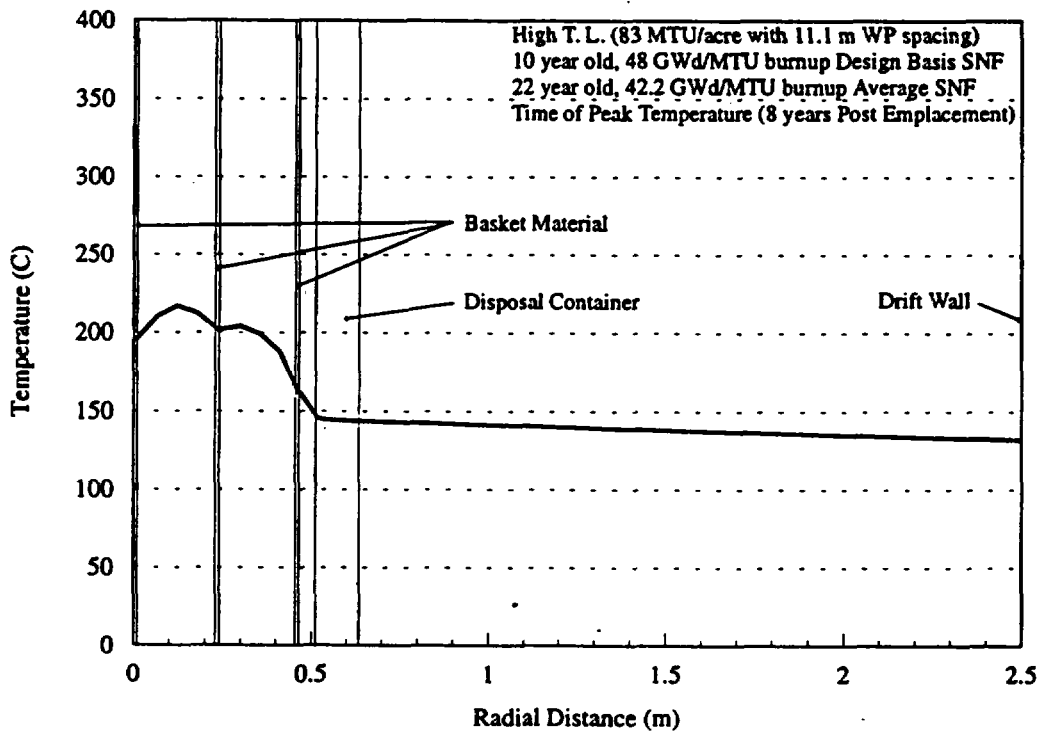
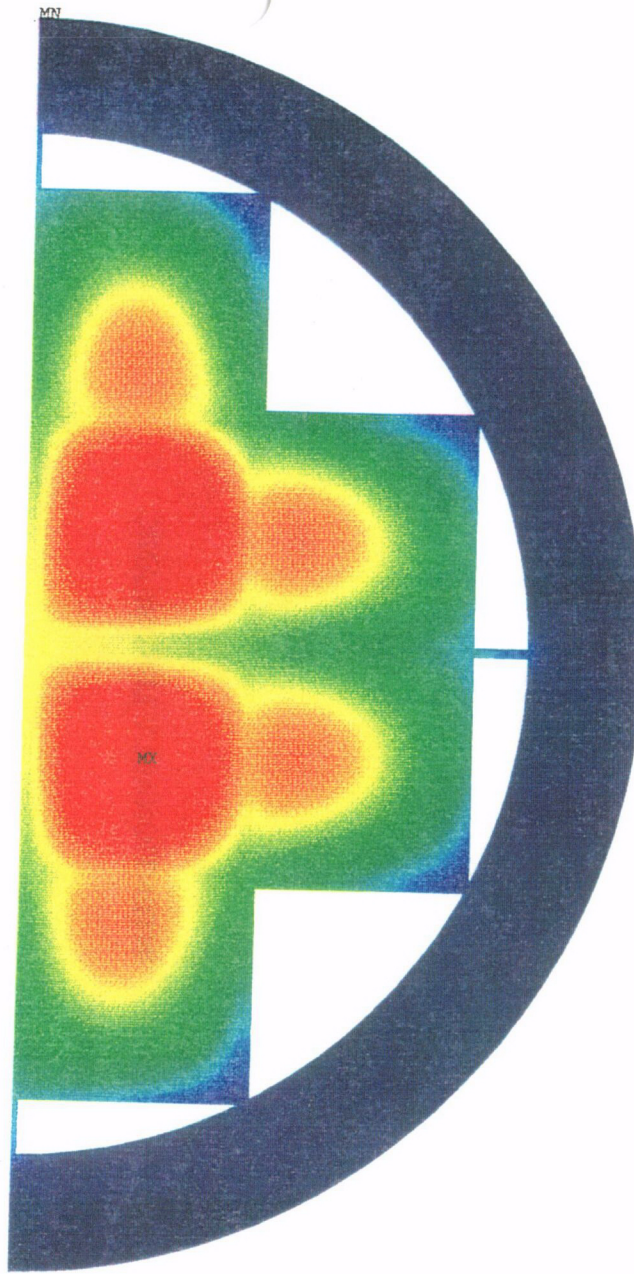


Figure 6.3-12. Temperature Profile in 12 PWR UCF

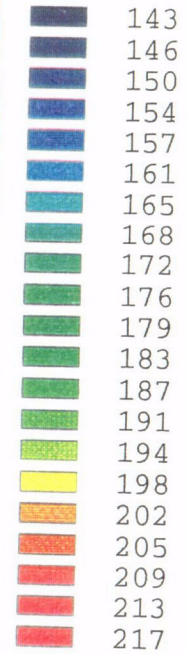


ANSYS 5.0 A
JUN 28 1995

Temperature

Min =142

Max =217



Degrees C

83 MTU/acre

10 year old SNF

48 GWd/MTU

C25

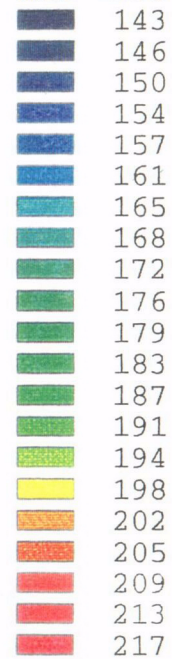
Figure 6.3-13. 12 PWR MPC Peak Temperatures (10 Years)

ANSYS 5.0 A
JUN 28 1995

Temperature

Min = 159

Max = 198



Degrees C

83 MTU/acre

10 year old SNF
48 GWd/MTU

C 26

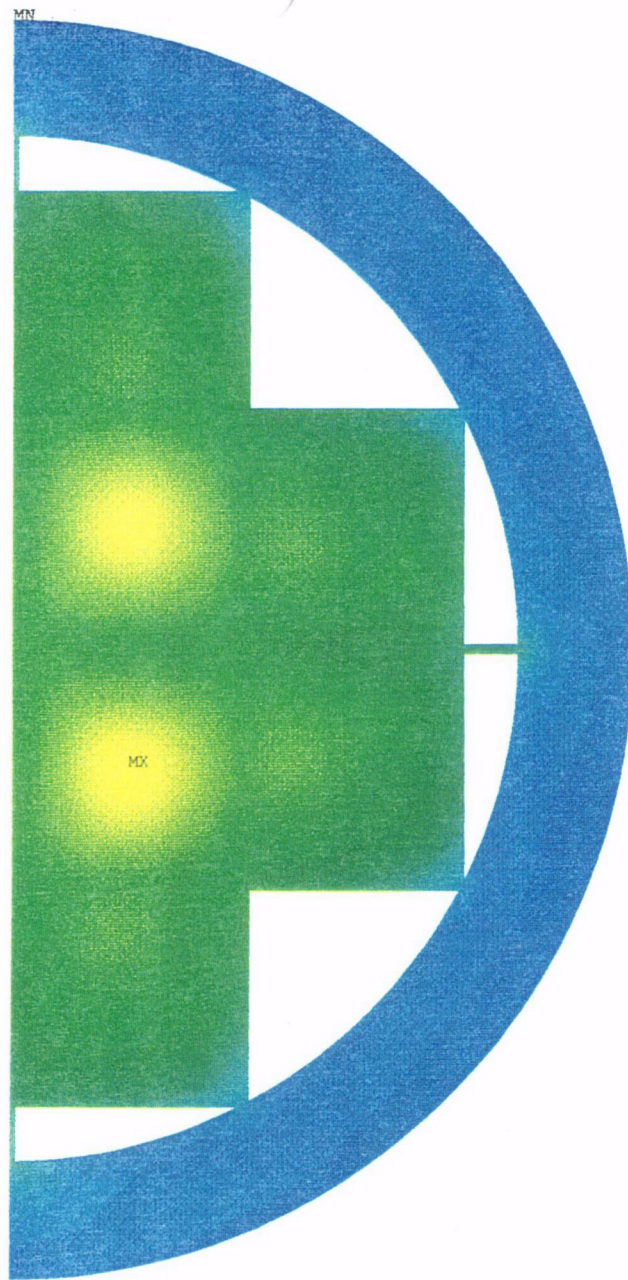
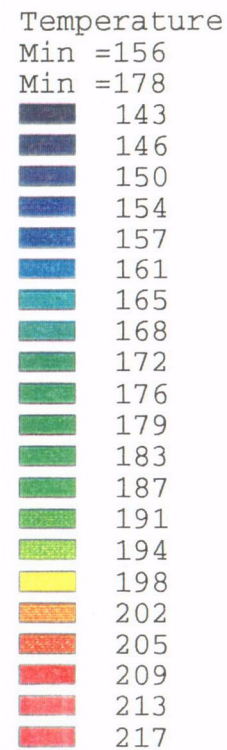
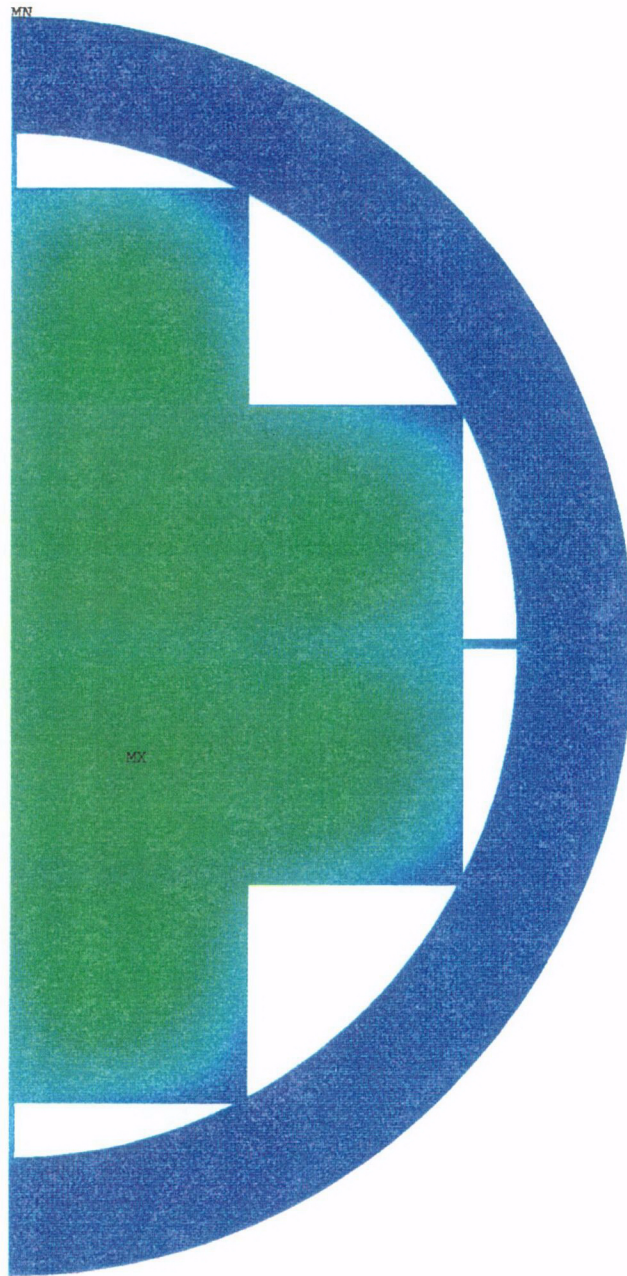


Figure 6.3-14. 12 PWR UCF Temperatures at 50 Years

ANSYS 5.0 A
JUN 28 1995



Degrees C

83 MTU/acre C 27

10 year old SNF
48 GWd/MTU

Figure 6.3-15. 12 PWR UCF Temperatures at 100 Years

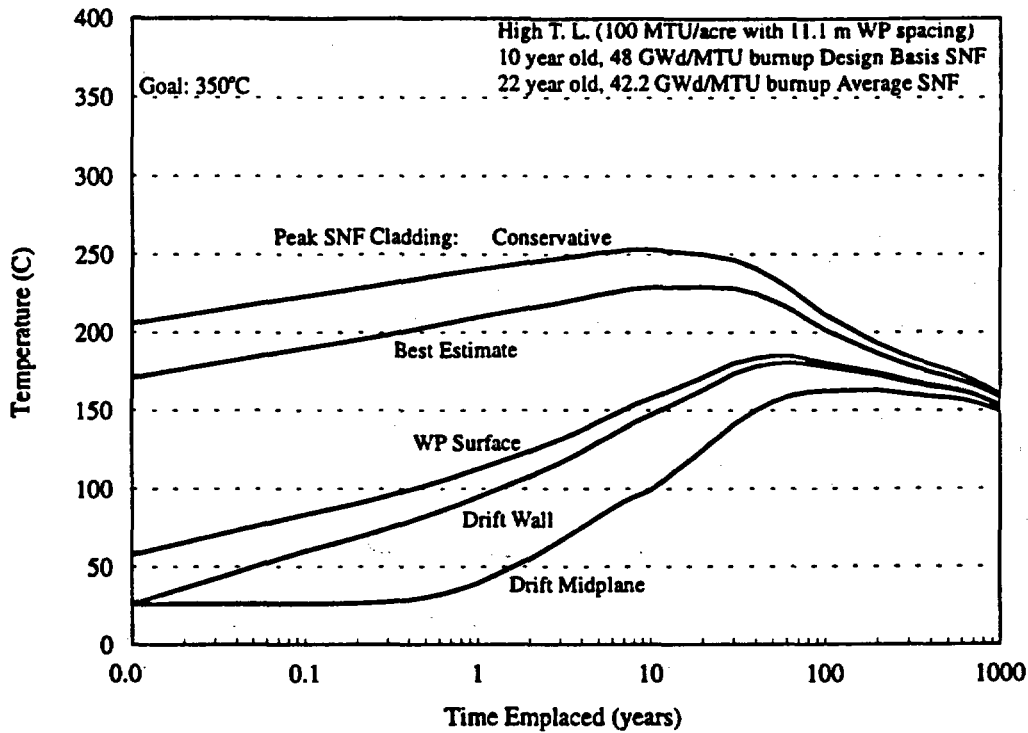


Figure 6.3-16. 12 PWR UCF, High Thermal Load (#1), MGDS DBF

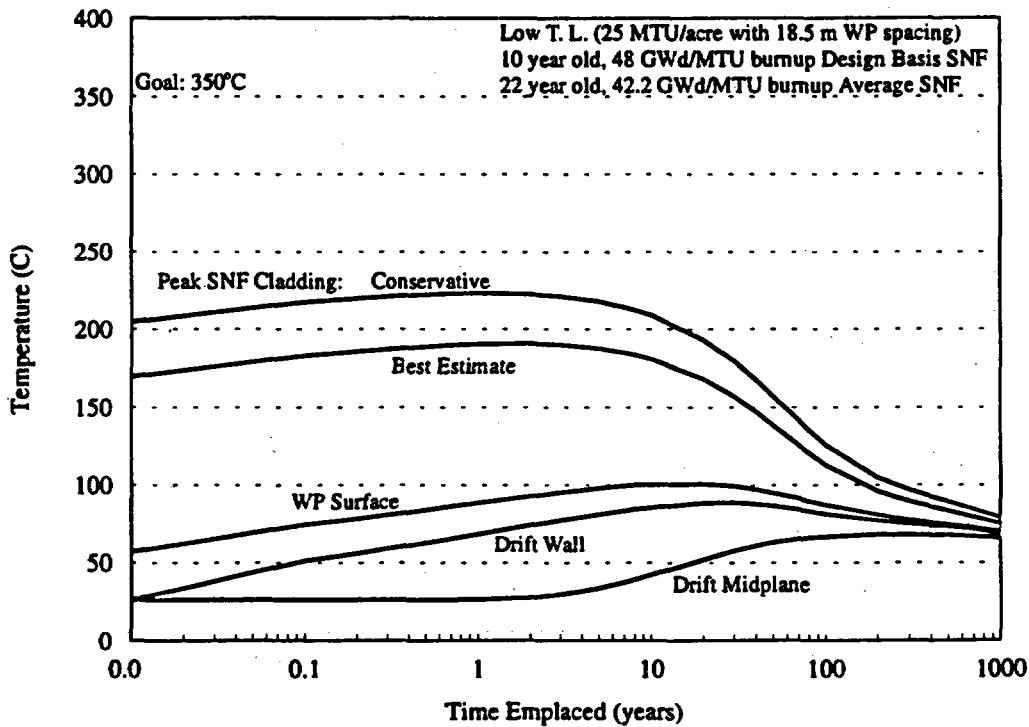


Figure 6.3-17. 12 PWR UCF, Low Thermal Load (#1), MGDS DBF

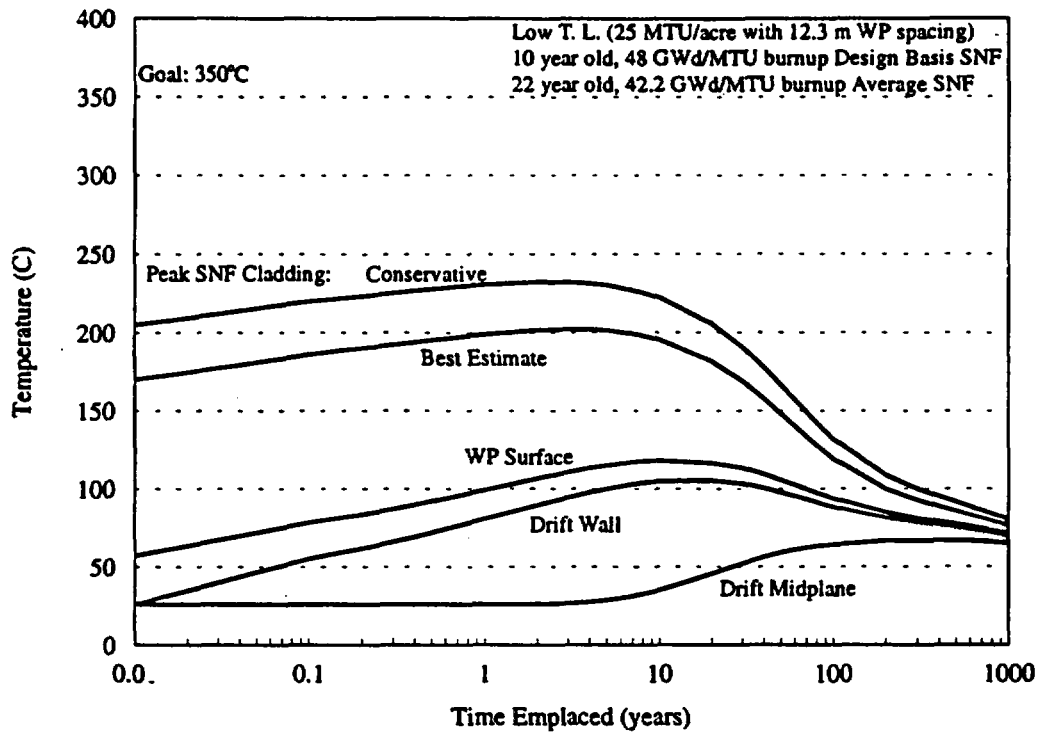


Figure 6.3-18. 12 PWR UCF, Low Thermal Load (#2), MGDS DBF

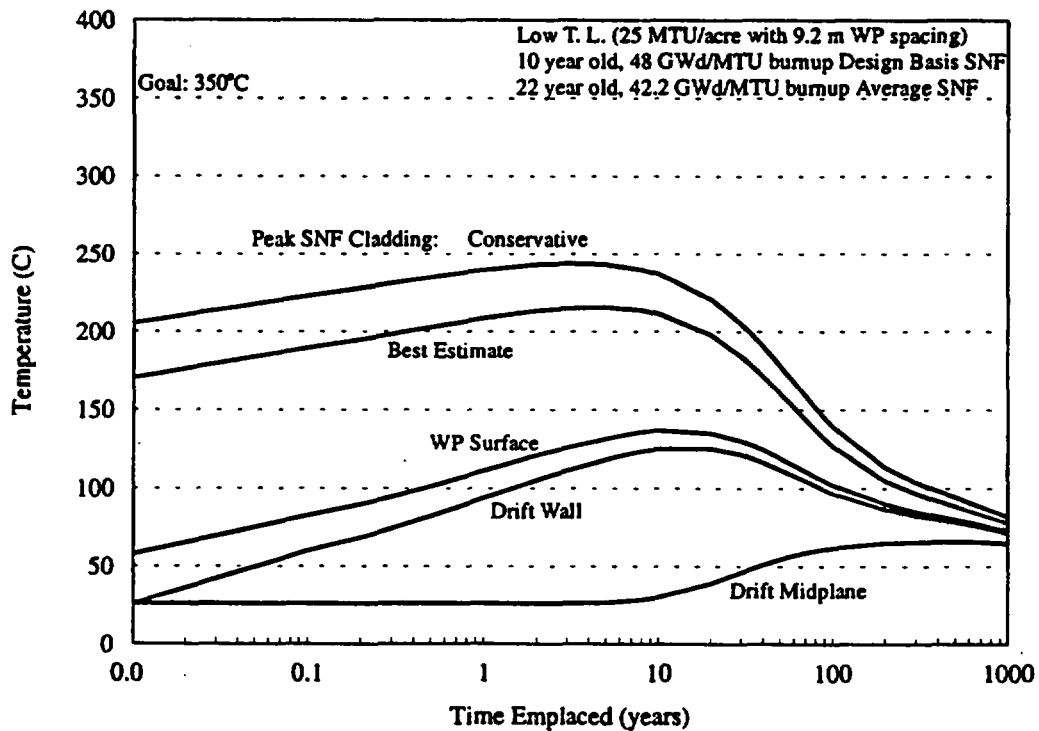


Figure 6.3-19. 12 PWR UCF, Low Thermal Load (#3), MGDS DBF